Physics – Uspekhi **64** (4) 370 – 385 (2021)

PHYSICS OF OUR DAYS

PACS numbers: 03.65.Ta, 42.65.Re, 78.47.J –

In search of lost time: attosecond physics, petahertz optoelectronics, and quantum speed limit

A M Zheltikov

DOI: https://doi.org/10.3367/UFNe.2020.11.038884

Contents

Abstract. Modern optical physics provides means to detect and resolve ultrafast processes on a time scale of tens of attoseconds. The physical interpretation of such measurements, however, remains the focus of heated debate. In its conceptual dimension, this debate reflects fundamental difficulties in defining time in quantum mechanics. En route toward resolving this difficulty, we are led to extend universal uncertainty relations to ultrafast light–matter interactions. Such a generalized uncertainty sets a lower bound on the response time inherent in attosecond electronic dynamics driven by ultrashort laser pulses, dictating a speed limit for next-generation photonic information systems — systems of petahertz optoelectronics.

Keywords: optical physics, ultrashort laser pulses, quantum mechanics, uncertainty relations

A M Zheltikov
Lomonosov Moscow State University, Physics Department,
Leninskie gory 1, 119991 Moscow, Russian Federation;
Institute for Quantum Science and Engineering,
Department of Physics and Astronomy,
Texas A&M University, College Station TX 77843, USA;
International Center for Quantum Optics and Quantum Technologies
(Russian Quantum Center),
ul. Bol'shoi bul'var 30, str. 1, 143025 Skolkovo, Moscow,
Russian Federation;
Tupolev Kazan National Research Technical University, KNRTU – KAI,
ul. Chetaeva 18, 420126 Kazan, Russian Federation;
National Research Center 'Kurchatov Institute',
pl. Akademika Kurchatova 1, 123182 Moscow, Russian Federation
E-mail: zheltikov@physics.msu.ru

Received 9 August 2020, revised 2 November 2020
Uspekhi Fizicheskikh Nauk **191** (4) 386 – 403 (2021)
Translated by A M Zheltikov

1. Introduction: attosecond electron dynamics, petahertz optoelectronics, and the problem of 'lost time' in quantum mechanics

Rapidly progressing methods of ultrafast optics open unique possibilities for time-resolved studies of ultrafast phenomena in atomic and molecular systems [1–10], solids [11–35], and biological systems [36]. As one of the most significant recent discoveries in this area, ultrafast photoionization was found to give rise to a unique regime of laser–matter interaction whereby a dielectric can be reversibly switched to a conducting state on the time scale of tens to hundreds of attoseconds [12, 13, 19, 37–40]. Spectral analysis of high-order harmonics generated as a part of this process has been shown to enable an all-optical detection of attosecond photoelectron pulses

produced via such photoionization and to provide a probe for attosecond electron wave-packet dynamics [15, 19, 20, 22, 23, 25, 28, 34, 35].

Experiments of the past few years open the routes toward unprecedented data-processing speeds, giving rise to a new optical technology — petahertz optoelectronics [37, 38]. Understanding the limitations on the performance of such systems requires a precise clocking of the laser-ionization-driven dielectric–conductor transition. The modern tool box of ultrafast optics provides means for adequately accurate time-resolved measurements on the time scale of 10–100 attoseconds [1–6, 16, 17, 41–49]. The time of photoionization is difficult to define not because of technical, but, rather, because of conceptual problems. These problems reflect the fundamental difficulties of the definition of time in quantum mechanics [50–60].

In its canonical version, quantum mechanics has no time operator in its repertoire, nor does it offer any consistent recipe to define time in terms of a quantum-mechanical expectation value. Quantum dynamics is a result of interference of an infinite manifold of 'prehistories,' which can be viewed as quantum paths. However, a quantum-path view of tunneling photoionization leads to a purely imaginary photoionization time. Imaginary time plays an important role in different physical settings [61–63], including a broad class of problems in thermodynamics and cosmology [64–67]. Whether or not this concept can help understand the photoionization time is open to debate, making many of time-resolved photoionization studies open to reinterpretation. The initial optimism regarding such measurements gives way to more cautious assessments. Below, we provide a review of some of the breakthroughs, new ideas, most significant achievements, and the main difficulties in this rapidly growing area of modern physics.

2. The hard problem of time in quantum mechanics: quantum jumps, uncertainty relations, and Pauli's theorem

Serious difficulties in the definition of time have been realized already in early days of quantum mechanics [68, 69]. We find it instructive to briefly summarize the main arguments related to the notion of time that the founders of quantum physics have put forward in early-era debates about the principles of quantum physics as these arguments have helped expose the central difficulties of the definition of time in quantum mechanics and outlined the horizons of the quantum theory of time-resolved measurements for the forthcoming century.

2.1 Bohr's theory, quantum jumps, and uncertainty of time measurements

Debates on time start to heat up right after the publication of the 1913 'quantum trilogy' by Bohr [70–72]. Rutherford and Slater object to Bohr's idea of 'quantum jumps' between electron orbitals that give rise to emission and absorption of radiation by atoms. They point out that the idea of quantum jumps is inconsistent with the properties of atomic absorption and emission spectra with their signature narrow spectral lines. In search for the ways out of this conundrum, Einstein resorts to a statistical description of atomic spectra in terms of probabilities of electronic transitions [73]. Heisenberg searches for the solution in the framework of matrix mechanics, which abandons the whole concept of electron orbitals. In his 1927 *Zeitschrift für Physik* paper [74], he proposes a new approach to the notion of time in quantum mechanics. From the perspective of this approach, the instant of time at which a system makes a quantum transition changing its energy by ΔE can only be resolved with an uncertainty $\Delta\tau \sim \hbar/(2\Delta E)$. Heisenberg also suggests an operator relation between the time and energy,

$$\mathbf{Et} - \mathbf{tE} = -\mathrm{i}\hbar\,. \tag{1}$$

He does not specify, however, the form of **E** and **t**, nor does he discuss whether an operator of time can be defined at all.[1] A year later, in his 1928 *Nature* paper [75], Bohr, with a reference to "relations well known from the theory of optical instruments," arrives at

$$\Delta t \Delta E = h\,, \tag{2}$$

interpreting ΔE as "the highest possible accuracy in the definition of energy ... associated with the wave-field."

In the years and decades to come, the uncertainty relation between energy and time expressed in the form of Eqn (2) will become one of the central points in a debate on the meaning of time in quantum dynamics and quantum measurements. The energy–time uncertainty relation would be then re-thought and re-interpreted a multiple number of times in the course of this debate, remaining one of the central pressing questions in quantum physics that still need to be resolved.

2.2 Pauli's theorem

As one of the milestones in the early debate on time in quantum theory, Pauli, as a part of his critique of the Heisenberg and Bohr arguments, comes up with a proposition [76] that later became known as Pauli's theorem. Pauli points out that that no unitary Hermitian energy shift operator $\hat{T}$ can be defined for Hamiltonians $\hat{H}$ whose discrete eigenvalue spectra are bounded from below. Because it rules out the existence of Hermitian $\hat{T}$ for a certain class of Hamiltonians, Pauli's argument has long been understood as a fundamental no-go for time as a quantum-mechanical observable, relegating time to the role of a parameter that cannot be represented in the operator form.

In modern quantum mechanics, however, Pauli's theorem is viewed [68, 69, 77] not as a total prohibition of the time operator, but rather as a limitation on the class of Hamiltonians that allow, in principle, the existence of such an operator. Indeed, provided that for any $\varepsilon \in \mathbb{R}$,

$$\exp\left(\frac{\mathrm{i}\varepsilon\hat{T}}{\hbar}\right)\hat{H}\exp\left(-\frac{\mathrm{i}\varepsilon\hat{T}}{\hbar}\right) = \hat{H} + \varepsilon\hat{I}\,, \tag{3}$$

the spectrum of eigenvalues of $\hat{H}$ should span the entire $\mathbb{R}$. While this result is fully consistent with Pauli's theorem, it does not imply, however, that a consistent definition of the time operator is completely forbidden. It does not rule out, for example, the existence of Hermitian time operators for Hamiltonians with unbounded spectra or spectra consisting of countably infinite sets of eigenvalues [78]. In some cases, non-Hermitian time operators may also prove possible and even productive [68, 69].

[1] Here, we keep the Heisenberg notations for **E** and **t** [74] by writing them in boldface. In what follows, whenever necessary for clarity, operators will be labeled with 'hats,' in line with contemporary textbook notation.

3. Faces of time in quantum mechanics

3.1 Internal and external time

As an important starting point, we need to figure out what role is assigned to the time in a specific physical setting. In quantum mechanics, time has more than one assignment. In the equations of quantum dynamics, time appears as a variable that clocks the evolution of a quantum system. When serving in this capacity, time plays the role of an external parameter, read out from an external, laboratory clock (Fig. 1a), and is often referred to as external or laboratory time [68, 69]. External time is disconnected from the dynamic variable of the quantum system and commutes with operators representing such dynamic variables.

It is the external time that the Heisenberg- and Bohr-type energy–time uncertainty relations can connect to,

$$\Delta t \Delta E \gtrsim \frac{\hbar}{2}\,, \tag{4}$$

with ΔE understood as the minimal error of energy measurements performed within a time interval Δt.

Time t is read out in quantum mechanics via sequential measurements on a dynamic variable A (Fig. 1b), represented by a time-dependent operator $\hat{A}$, which generally evolves in time as $\hat{A}(t)$. The time found by solving quantum evolution equations for $\hat{A}(t)$ can be represented as an operator $\hat{T}$, expressed via $\hat{A}(t)$. Such time is often referred to as the internal time [68, 69].

The notion of internal time entails a vast variety of energy–time uncertainty relations similar to Eqn (4). The content of $\Delta\tau$ in such relations is, however, distinctly different from $\Delta\tau$ in the inequalities of the form (4) for the external time. In energy–time uncertainty relations for the internal time, $\Delta\tau$ is understood as a fundamentally unavoidable uncertainty of time as dictated by quantum uncertainty relations, as opposed to instrumental errors and apparatus functions. Important examples of such relations are discussed in Section 4.

3.2 Time as a quantum observable and the time operator

Finding a suitable operator for internal time T is often difficult and not solvable within the class of friendly, closed-form $\hat{T}$ operators. To illustrate these difficulties, we follow the treatment of Peres [79] and consider a free particle with a momentum p and mass m. The Hamiltonian of such a particle is $H = p^2/(2m)$. Introducing $T = mq/p$, where q is the space coordinate, we find for the Poisson bracket of T and H: $\{T, H\} = 1$. The operator T is thus a natural choice for the internal time, providing a convenient clock for a classical free particle.

In quantum mechanics, this simple and natural definition of the time operator runs into difficulties. Quantum extension of $T = mq/p$ leads to [79]

$$T = \mathrm{i}\,\frac{\hbar m}{2}\left(\frac{1}{p}\frac{\partial}{\partial p} + \frac{\partial}{\partial p}\frac{1}{p}\right). \tag{5}$$

Such an operator obeys the commutation relation $[T, H] = \mathrm{i}\hbar$, as necessary. Solving for the eigenfunctions of the equation $T\psi = t\psi$ yields

$$\psi \sim \sqrt{p}\,\exp\left(-\mathrm{i}\,\frac{p^2}{2m\hbar}\,t\right). \tag{6}$$

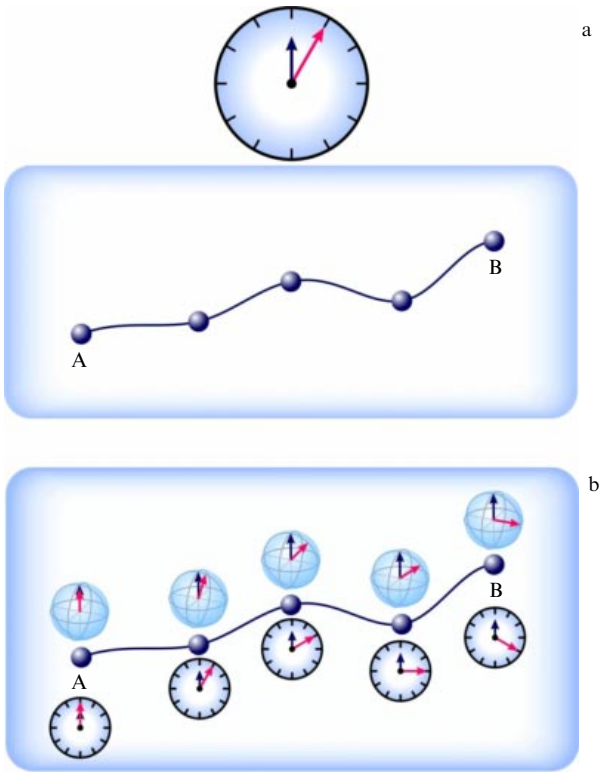

Figure 1. (Color online.) (a) Internal and (b) external time in quantum mechanics.

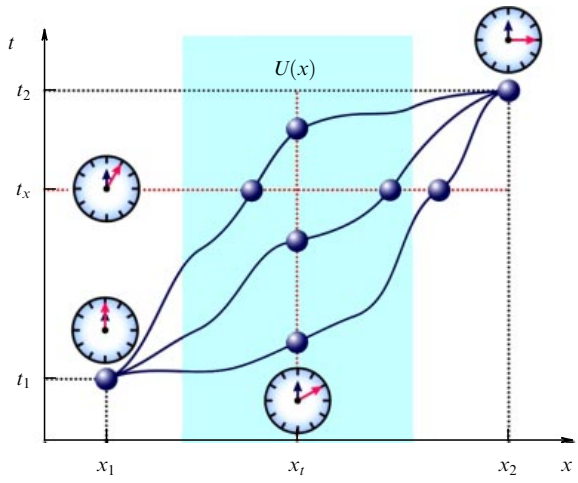

Figure 2. (Color online.) Quantum evolution as an interference of prehistories — quantum paths. The range of the potential $U(x)$, Ω, is shown with shading.

As can be seen from Eqns (5) and (6), neither the T operator nor its eigenfunctions allow any physically clear interpretation, offering no physically transparent method of measurements. Thus, in questions related to the definition of time, solutions based on straightforward classical analogies fail even for systems as simple as a free particle.

Especially difficult are the questions related to the definition of time for quantum processes that have no classically analogs, such as a tunneling of quantum particles through potential barriers. In search for the duration of the time interval τ that a quantum particle spends in the region Ω under the potential barrier (Fig. 2), we represent the wave

function $\psi(x,t)$ in the form of an integral [54–58]

$$\psi(x,t)=\int_0^t \Phi(x,t|\tau)\,\mathrm{d}\tau\,. \tag{7}$$

The functions $\Phi(x,t|\tau)$ in the expansion (7) represent the subset of trajectories for which the time that the particle spends in Ω is exactly τ,

$$\Phi(x,\eta|\tau)=\int \mathrm{d}\xi \int_{\xi(0);\,x(\eta)} Dx(t)\,\delta\bigl(\tau_\Omega[x(t)]-\tau\bigr) \times \exp\left\{\mathrm{i}\,\frac{S[x(t)]}{\hbar}\right\}\psi(\xi,0)\,,$$

where $S[x(t)]=\int_0^\eta [m\dot{x}^2/2-U(x)]\,\mathrm{d}t$, $Dx(t)$ is the sum over all the trajectories starting at $(\xi,0)$ and terminating at (x,η), $\tau_\Omega[x(t)]=\int_0^\eta \Theta_\Omega(x(t))\,\mathrm{d}t$, and $\Theta(x)=1$ for $x\in\Omega$ and $\Theta(x)=0$ for $x\notin\Omega$.

Since the wave function $\psi(x,t)$ is the solution to the Schrödinger equation, $\Phi(x,t|\tau)$ meets the equation

$$\mathrm{i}\hbar\,\frac{\partial\Phi(x,t|\tau)}{\partial t}=-\frac{\hbar^2}{2m}\,\frac{\partial^2\Phi(x,t|\tau)}{\partial x^2}+U(x)\psi(x,t) -\mathrm{i}\hbar\Theta_\Omega(x)\,\frac{\partial\Phi(x,t|\tau)}{\partial\tau}\,.$$

It can now be seen that Eqn (7) sorts particle trajectories in times τ. The state of a particle at a point x_2 at the moment of time t_2 is thus represented as the sum of an infinite number of interfering 'prehistories' (see Fig. 2). Similar to the celebrated double-slit diffraction, where the number of interfering trajectories is two, detection of individual trajectories destroys the interference pattern, that is, $\psi(x,t)$. The overall wave function $\psi(x,t)$, on the other hand, does not offer means to resolve individual $\Phi(x,t|\tau)$. Information on individual quantum trajectories, each representing a well-defined τ, is lost. The answer to the question of how long the tunneling time is thus cannot be answered without answering the question of how the measurement is performed (see Fig. 2). The reading of the clock whose location is fixed in space, $\mathbf{r}=\mathbf{r}_t$, will differ from the reading of the clock read out at a fixed moment of time, $t=t_{\mathbf{r}}$.

3.3 Delay time

The time delay operator is an important example of a consistently defined Hermitian operator that can adequately represent a physical quantity related to time in quantum mechanics. The idea of this operator traces back to the arguments put forth by Eisenbud [80], Bohm [81], and Wigner [82], suggesting that, for a wave packet with a phase φ, the delay time Δt can be defined via the derivative of the phase in energy or momentum:

$$\Delta t_{\mathrm{ph}}=\frac{m_\mathrm{e}\hbar}{p_0}\left(\frac{\partial\varphi}{\partial p}\right)_{p=p_0}\,, \tag{8}$$

where m_e is the electron mass and p_0 is the momentum corresponding to the center of the wave packet.

Applied to the scattering matrix $\hat{S}(E)$ considered as a function of time, this relation between the delay time and the phase of a wave packet allows a self-adjoint delay time operator to be defined as [59, 83]

$$\hat{T}=-\mathrm{i}\hbar\hat{S}^{-1}\,\frac{\mathrm{d}\hat{S}}{\mathrm{d}E}=\hat{T}^\dagger\,. \tag{9}$$

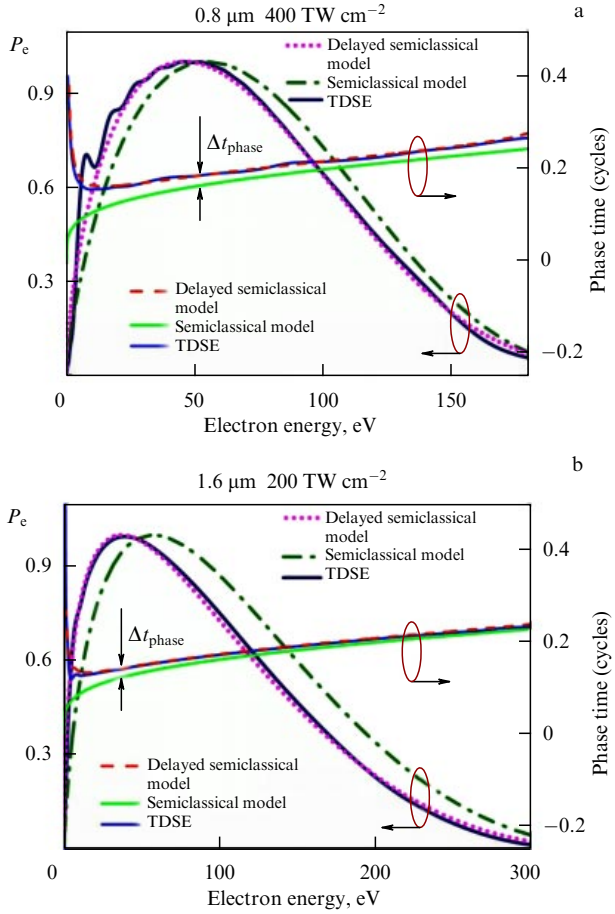

Figure 3. (Color online.) The electron energy distribution function (left axis) and the phase delay time (right axis) calculated by solving the time-dependent Schrödinger equation (blue and navy solid lines) and using the semiclassical model with (pink dotted and red dashed lines) and without (dash–dotted and solid green lines) correction for the delay due to the interaction with the potential of the atomic core. The central wavelength of the laser pulse is 0.8 μm (a) and 1.6 μm (b). The peak intensity of the laser pulse is 400 TW cm^{-2} (a) and 200 TW cm^{-2} (b).

Delay time defined in accordance with Eqn (9) proves useful for a vast class of quantum dynamics problems. Figures 3a and 3b present the numerical solution [84] of the time-dependent Schrödinger equation (TDSE) for the energy distribution function of photoelectrons produced via ionization of a hydrogenlike atom with a linearly polarized laser field. The z-axis in these simulations is chosen along the laser field and the energy of photoelectrons, ε, is shown along the abscissa axis in Figs 3a and 3b. The photoelectron energy distribution function in Figs 3a and 3b is found by solving the TDSE for a wave packet of tunneling photoelectrons of the form $\psi_f(\mathbf{r},t)=|\psi_f(\mathbf{r},t)|\exp[\mathrm{i}\eta(\mathbf{r},t)]$. The phase delay of this wave packet is calculated as $\Delta t_{\mathrm{ph}}(\varepsilon)=m_\mathrm{e}/(\hbar p_z)\partial\tilde{\eta}(p_z)/\partial p_z$, where $\tilde{\eta}(p_z)$ is the phase of the momentum-space wave function $\tilde{\psi}_f(p_z,t)$, found as a momentum representation of $\psi_f(\mathbf{r},t)$, with p_z being the z-component of the photoelectron momentum.

The right axis in Figs 3a and 3b presents the phase time as a function of the photoelectron energy, ε, found by solving the TDSE and by using the semiclassical model of a laser-driven electron wave packet [85, 86]. The discrepancy between the predictions of the fully quantum and semiclassical models is almost entirely due to an extra phase delay induced by the

interaction of electrons with the potential of the parent ion [87]. With adequate corrections for this extra phase delay, the agreement between the semiclassical and fully quantum models is radically improved (Figs 3a, b).

4. Mandelstam–Tamm uncertainty relation

The paper "The uncertainty relation between energy and time in nonrelativistic quantum mechanics," published by Mandelstam and Tamm in the spring of 1945 [88],[2] is one of the most significant milestones along the way toward understanding the fundamental quantum uncertainty of time. All the earlier energy–time uncertainty relations were postulated either without any proof or by analogy with other uncertainty relation, such as the position–momentum uncertainty or uncertainties as dictated by the properties of the Fourier transform, known in signal analysis [89– 91].

Mandelstam and Tamm have shown in their 1945 paper [88] that energy–time uncertainty relations can be derived via a rigorous analysis of quantum evolution equations. Although the relations obtained by such an analysis can take the form of Eqn (2) or (4), their physical content is much deeper. The Mandelstam–Tamm uncertainty relations extend well beyond the uncertainty of energy and time measurements. Among their most important corollaries, these relations lead to a realization of the fundamental upper bound for the rate of quantum evolution, quantum information processing, and quantum communication.

As an introduction to their work, Mandelstam and Tamm offer their critique of the energy–time uncertainty relation in the form of Eqn (2),[3] pointing out that, at the time of their writing, this relation did not have any rigorous justification or proof. "In nonrelativistic quantum mechanics, the energy can be treated as an observable,[4] in Dirac's sense, corresponding to the Hamilton operator of a mechanical system. When defined this way, the energy is, of course, not identical to the frequency of a monochromatic oscillation times h. The aforesaid justification thus loses its validity, while Eqn (2) ceases to be meaningful... At the time of this writing, there seems to be no general justification of Eqn (2) or any other similar uncertainty relation concerning the energy that would be based on the fundamental principles of quantum mechanics."

Analysis provided by Mandelstam and Tamm is based on the evolution equation for an operator $\hat{R}$ representing a physical observable,

$$\frac{\partial \hat{R}}{\partial t} = \frac{\mathrm{i}}{\hbar}[\hat{H}, \hat{R}]\,, \tag{10}$$

where $\hat{H}$ is the stationary Hamiltonian, i.e., the Hamiltonian that does not depend on time explicitly.

Since for any $\hat{R}$ and $\hat{S}$

$$\Delta S \Delta R \geqslant \frac{1}{2}\left|\langle[\hat{S}, \hat{R}]\rangle\right|, \tag{11}$$

where $(\Delta O)^2 = \langle \hat{O}^2\rangle - \langle\hat{O}\rangle^2$, Eqn (10) leads to

$$\Delta H \Delta R \geqslant \frac{\hbar}{2}\left|\left\langle\frac{\partial \hat{R}}{\partial t}\right\rangle\right|. \tag{12}$$

[2] This paper was published in a special issue of *Izv. Akad. Nauk SSSR, Ser. Fiz.*, dedicated to the memory of academician L I Mandelstam (1879–1944).
[3] Equation (2) in the Mandelstam and Tamm paper is the same as Eqn (2) in this review.
[4] In English in the original.

Inequality (12) can be rewritten in the form of an energy–time uncertainty relation:

$$\tau_R |\Delta H| \geqslant \frac{\hbar}{2}\,, \tag{13}$$

where

$$\tau_R = |\Delta R|\left|\left\langle\frac{\partial \hat{R}}{\partial t}\right\rangle\right|^{-1}. \tag{14}$$

Inequality (13) is one of the widely recognized forms of the Mandelstam–Tamm uncertainty relation. However, the analysis that Mandelstam and Tamm present in their 1945 paper [88] is not limited to the derivation of this relation. They proceed by considering a projection operator defined by

$$\hat{L}\psi = (\psi_0\psi)\psi_0\,, \tag{15}$$

where

$$(\psi_0\psi) = \int \psi_0^*\psi\,\mathrm{d}x\,. \tag{16}$$

Since one of the eigenvalues of $\hat{L}$ is 1, while all the other are equal to zero, the expectation value of this operator, $\langle\hat{L}\rangle$, meets the inequality $\langle\hat{L}\rangle \leqslant 1$. Combining this result with Eqn (12) yields

$$\Delta H\left[\langle\hat{L}\rangle - \langle\hat{L}\rangle^2\right]^{1/2} \geqslant \frac{h}{2}\left|\frac{\mathrm{d}\langle\hat{L}\rangle}{\mathrm{d}t}\right|.$$

We now assume that, at the initial moment of time, the system is in the state ψ_0, that is, $\langle\hat{L}(0)\rangle = 1$. We can then integrate the inequality above for $t \geqslant 0$ to find

$$\frac{\pi}{2} - \arcsin\left(\langle\hat{L}\rangle^{1/2}\right) \geqslant \frac{\Delta H}{\hbar}\,t\,. \tag{17}$$

It is convenient to rewrite this relation as

$$\langle\hat{L}\rangle \geqslant \cos^2\left(\frac{\Delta H}{\hbar}\,t\right). \tag{18}$$

Representing the states ψ_0 and $\psi_t = \psi$ as state kets $|\psi(0)\rangle$ and $|\psi(t)\rangle$ and defining the angle between these kets (Fig. 4) as

$$\vartheta(\psi_0, \psi_t) = \arccos\left(\left|\langle\psi_0|\psi_t\rangle\right|\right), \tag{19}$$

we arrive at the following uncertainty relation:

$$\left|\frac{\mathrm{d}\vartheta}{\mathrm{d}t}\right| \leqslant \frac{\Delta H}{\hbar}\,. \tag{20}$$

We can now use Eqn (20) to find that the time τ required for a quantum system initially residing in a state $|\psi(0)\rangle$ to evolve to a state $|\psi(\tau)\rangle$ orthogonal to $|\psi(0)\rangle$, such that $\langle\psi(0)|\psi(\tau)\rangle = 0$, meets the following inequality:

$$\tau \geqslant \tau_{\mathrm{MT}} \equiv \frac{\pi}{2}\,\frac{\hbar}{\Delta H} = \frac{\pi}{2}\,\frac{\hbar}{\Delta E}\,, \tag{21}$$

where

$$(\Delta E)^2 = (\Delta H)^2 = \langle\hat{H}^2\rangle - \langle\hat{H}\rangle^2\,. \tag{22}$$

Inequality (21) can be represented in a form similar to Eqn (2), that is, in the form of the Heisenberg and Bohr

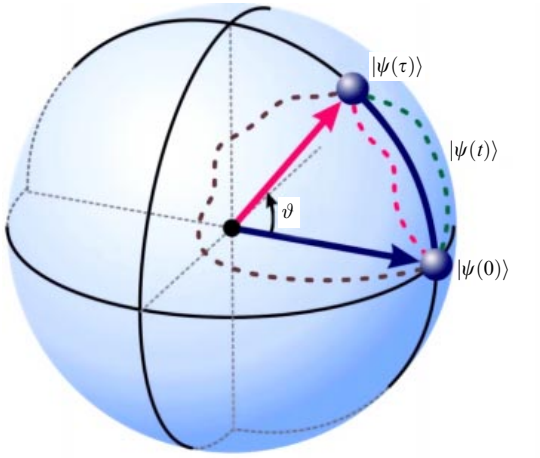

Figure 4. (Color online.) The initial state ket, $|\psi(0)\rangle$, and the state kets at the current and final moments of time, $|\psi(t)\rangle$ and $|\psi(\tau)\rangle$. Also shown are the segment of the geodesic line connecting the initial and final states of the system (solid line) and quantum paths corresponding to the actual evolution of the system (dashed lines).

uncertainty relations [74, 75] used as an argument in the Bohr–Einstein debates. However, in its physical and formally mathematical content, Eqn (21) is distinctly different from Eqn (2). In Eqn (21), the energy uncertainty ΔE is no longer the highest accuracy of energy reading, but is a measure of the Hamiltonian variance. As one of its key insights, analysis by Mandelstam and Tamm relates quantum uncertainty to the physical limit on the rate of quantum dynamics.

5. Quantum fidelity and quantum speed limit

Equation (20) suggests a physical quantifier for the physical similarity of quantum states ψ_0 and ψ_t at a given moment of time. For pure quantum states, this quantifier, referred to as the quantum fidelity, is defined as [92, 93]

$$F(\psi_0, \psi_t) = \left|\langle\psi_0|\psi_t\rangle\right|^2 . \tag{23}$$

As can be seen from Eqns (19)–(21), for $0 \leqslant \Delta H t/\hbar \leqslant \pi/2$, the function $F(\psi_0, \psi_t)$ meets the inequality

$$F(\psi_0, \psi_t) \geqslant \cos^2\left(\frac{\Delta H}{\hbar}\, t\right) . \tag{24}$$

The evolution time τ required for the system to reach a state ψ_τ whose fidelity to ψ_0 does not exceed $F(\psi_0, \psi_\tau)$ is bounded from below by

$$\tau \geqslant \frac{\hbar}{\Delta H} \arccos\left\{\left[F(\psi_0, \psi_t)\right]^{1/2}\right\} . \tag{25}$$

The Mandelstam–Tamm treatment thus not only provides a rigorous quantum-mechanical justification of the energy–time uncertainty relation, but also reveals the fundamental physical limit on the evolution rate of parameters in a quantum system, setting this limit at the lower bound on the uncertainty as defined by Eqns (14) and (21),

$$w_0 = \frac{1}{\tau_0} = \frac{1}{\tau_{\mathrm{MT}}} . \tag{26}$$

Viewed in the context of quantum information processing and quantum communication, Eqn (26) defines a 'quantum speed limit' [93–101],

$$\tau_{\mathrm{QSL}} = \tau_{\mathrm{MT}} , \tag{27}$$

suggesting the means for 'quantum control' [102] — quantum Hamiltonian engineering. Quantum control studies reveal important properties of the quantum speed limit for a broad range of physical parameters and a vast variety of quantum information processing and quantum communication settings. These findings offer deeper insights into the manifestations of energy–time uncertainty [100–102].

6. Energy–time uncertainty for systems with time-dependent Hamiltonians

Mandelstam–Tamm analysis is performed for a quantum system whose quantum dynamics is governed by a stationary Hamiltonian $\hat{H}$. Because of this limitation, the Mandelstam–Tamm energy–time uncertainty relation, at least in its original form, cannot be directly extended to a broader class of problems, including the problems of laser–matter interaction, where a description of quantum dynamics requires a time-dependent Hamiltonian, $\hat{H}_t$. As one of the central difficulties of such an extension [103], for a system with a time-dependent Hamiltonian $\hat{H}_t$, the evolution operator $\hat{U}_t$ can no longer be represented as

$$\hat{U} = \exp\left(-\mathrm{i}\,\frac{\hat{H}}{\hbar}\, t\right) . \tag{28}$$

When the Hamiltonian is time-dependent, the right-hand side of Eqn (28) is only the first term in the expansion [104]:

$$\hat{U}_\tau = \exp\left(-\mathrm{i}\,\frac{\hat{\Omega}_\tau}{\hbar}\right) , \tag{29}$$

$$\hat{\Omega}_\tau = \int_0^\tau \mathrm{d}t_1\, \hat{H}_{t_1} - \frac{\mathrm{i}}{2\hbar}\int_0^\tau \mathrm{d}t_1 \int_0^{t_1} \mathrm{d}t_2\, [\hat{H}_{t_1}, \hat{H}_{t_2}] + \ldots . \tag{30}$$

A formal generalization of the Mandelstam–Tamm uncertainty relation to a system with such a Hamiltonian leads to [103]

$$\tau \geqslant \frac{\hbar}{\Delta\tilde{E}_\tau}\, \vartheta(\psi_0, \psi_\tau) , \tag{31}$$

where $\Delta\tilde{E}_\tau$ is given by

$$\Delta\tilde{E}_\tau = \frac{1}{\tau}\left|\langle\psi_0|\hat{\Omega}_\tau|\psi_0\rangle\right| . \tag{32}$$

Nominally, Eqn (31) has the form of the Mandelstam–Tamm energy–time uncertainty relation. Equation (32), however, does not give any simple and clear recipe for the calculation of $\Delta\tilde{E}_\tau$ and is therefore rather formal. Except for a few special cases, including the case of adiabatic quantum evolution (see, e.g., [103]), such a recipe has not been found so far. In Section 7, we will provide a more detailed discussion of the difficulties encountered in the generalization of the Mandelstam–Tamm uncertainty relation to systems with time-dependent Hamiltonians. Based on the analysis of laser-driven quantum dynamics [105–107], we will show that whether or not a meaningful energy–time uncertainty relation can be formalized for a given Hamiltonian depends not only on the form of the Hamiltonian, but also on the regime of laser-field–quantum-system interaction.

7. Laser-driven quantum dynamics

We will now apply the methods and relations discussed in the previous sections to understand the limit τ_0^{-1} for the rate of quantum evolution driven by ultrashort laser pulses. With this aim in mind, we represent the governing Hamiltonian as

$$\hat{H}_t = \hat{H}_0 + \hat{V}(t)\,, \tag{33}$$

where $\hat{H}_0$ is the stationary Hamiltonian of the system in the absence of the laser field,

$$\hat{V}(t) = -e\mathbf{E}\mathbf{r}\sin(\omega t) \tag{34}$$

is the time-dependent part of the Hamiltonian, describing the electric-dipole coupling of the quantum system with a dipole moment $\mathbf{d} = -e\mathbf{r}$ to an electromagnetic field with an amplitude $\mathbf{E} = \mathbf{E}(t)$ and frequency ω.

We consider the evolution of a quantum system that is initially, at $t = 0$, in a state $|\psi(0)\rangle = \psi_0$ and that obeys the Schrödinger equation

$$\mathrm{i}\hbar\,\frac{\partial}{\partial t}\,\big|\psi(t)\big\rangle = \hat{H}_t\big|\psi(t)\big\rangle\,. \tag{35}$$

According to the Pfeifer theorem [108], the population $q(t) = |\langle\varphi|\psi(t)\rangle|$ of an arbitrary quantum state φ is bounded at any moment of time $0 \leqslant t \leqslant T_\pm$ by

$$q_-(t) \leqslant q(t) \leqslant q_+(t)\,, \quad 0 \leqslant t \leqslant T_\pm\,, \tag{36}$$

where

$$q_\pm(t) = \sin\big(\delta \pm \chi(t)\big)\,, \tag{37}$$

$$\delta = \arcsin\big(\big|\langle\varphi|\psi_0\rangle\big|\big)\,, \tag{38}$$

$$\chi(t) = \frac{1}{\hbar}\int_0^t \min\{\Delta H_\varphi, \Delta H_{\psi_0}\}\,\mathrm{d}\vartheta\,, \tag{39}$$

$$(\Delta H_\psi)^2 = \big\langle\psi|\hat{H}_\vartheta^2|\psi\big\rangle - \big\langle\psi|\hat{H}_\vartheta|\psi\big\rangle^2\,, \tag{40}$$

$\psi_0 = \psi(0)$ is the initial state of the system, and $T_\pm$ are found from the equations $q_+(T_+) = 1$ and $q_-(T_-) = 0$.

Choosing $\varphi = \psi_0$, where $\psi_0 = \psi(0)$ is the initial state of the system, we find $\delta = \pi/2$. With such a choice of φ, the first inequality in Eqn (36) leads to [108]

$$\big|\big\langle\psi_0|\psi(t)\big\rangle\big| \geqslant q_-(t) = \cos\big[\Phi(t)\big]\,, \tag{41}$$

where

$$\Phi(t) = \frac{1}{\hbar}\int_{-\infty}^t \Delta H_{\psi_0}(\vartheta)\,\mathrm{d}\vartheta\,. \tag{42}$$

Inequality (41) sets a limit for the rate of evolution of a quantum system from the initial state ψ_0. Moreover, this inequality relates the maximum rate of such an evolution to the variance of the Hamiltonian in the state ψ_0. In this sense, inequality (41) extends the Mandelstam–Tamm energy–time uncertainty relation to the dynamics of a quantum system governed by a time-dependent Hamiltonian (33) with an interaction operator (34), typical of laser–matter interactions.

Unlike the canonical original version of the Mandelstam–Tamm uncertainty relation (21), valid for stationary Hamiltonians, inequality (41) operates with the time integral of the energy variance, $\Phi(t)$, rather than the energy variance itself. In a general case, Eqns (41) and (42) lead to a complicated nonlinear relation between the maximum rate of quantum evolution and the energy variance of the system in the initial state [109].

8. Uncertainty relations and the speed limit of electron dynamics

We now consider the case when the state ket $|\varphi\rangle$ is orthogonal to $|\psi(0)\rangle = \psi_0$. The second inequality in Eqn (36) then leads to the following limitation on the population rate [108, 110]:

$$\big|\big\langle\varphi|\psi(t)\big\rangle\big| \geqslant q_+(t) = \sin\big[\Phi(t)\big]\,. \tag{43}$$

As can be seen from Eqn (43), the population rate of the state whose state ket is orthogonal to the initial state ket is bounded. Similar to the speed limit of quantum evolution from state ψ_0, the maximum population rate of a state whose state ket is orthogonal to ψ_0 is determined by the time integral of the energy variance in the state ψ_0.

Suppose that, at the initial state, the quantum system is in a state that can be approximately described with the ground-state wave function of a hydrogenlike atom. Then, taking the field in the form of a linearly polarized pulse,

$$\mathbf{E}(t) = \mathbf{e}_0 E f(t)\sin(\omega t + \varphi_0)\,, \tag{44}$$

choosing the z-axis along $\mathbf{e}_0$, and taking into consideration that, for the ground state of the hydrogen atom, $\langle z\rangle_0 = 0$ and $\langle z^2\rangle_0 = \langle r^2\rangle_0/3 = a_0$, where a_0 is the radius of the first Bohr orbit, we find

$$\Delta H_{\psi_0}(\vartheta) = eEa_0 f(\vartheta)\big|\sin(\omega\vartheta + \varphi_0)\big|\,, \tag{45}$$

$$\Phi(t) = \frac{eEa_0}{\hbar}\int_{-\infty}^t f(\vartheta)\big|\sin(\omega\vartheta + \varphi_0)\big|\,\mathrm{d}\vartheta\,. \tag{46}$$

Alongside the time-dependent variance ΔH_{ψ_0}, it is instructive to consider the Hamiltonian variance averaged over the field cycle $T_0 = 2\pi/\omega$,

$$\Delta H_0 = \frac{1}{T_0}\int_0^{T_0} \Delta H_{\psi_0}\,\mathrm{d}\vartheta\,. \tag{47}$$

For ultrashort field waveforms (44) with a pulse width τ_0 on the order of the field cycle T_0, the variance ΔH_0 can no longer provide a meaningful measure for the mean energy variance. Yet, as will be shown below, even for very short field waveforms, the mean Hamiltonian variance as defined by Eqn (47) continues to serve as an important quantifier for the time scale of quantum dynamics.

For the ground state of a hydrogenlike atom, Eqn (47) leads to the following result for the Hamiltonian variance averaged over the field cycle T_0:

$$\Delta H_0 = \frac{4\hbar}{\gamma_\mathrm{K} T_0} = \frac{2\hbar}{\pi\tau_\mathrm{K}}\,, \tag{48}$$

where

$$\gamma_\mathrm{K} = \frac{\omega}{eE_0}\,(2m_\mathrm{e}I_0)^{1/2} \tag{49}$$

is the Keldysh parameter [111], I_0 is the field intensity, and

$$\tau_{\mathrm{K}} = \frac{\gamma_{\mathrm{K}}}{\omega} = \frac{(2m_{\mathrm{e}}I_0)^{1/2}}{eE_0}\,. \tag{50}$$

Following the terminology accepted in a vast literature on quantum tunneling [51, 52, 112, 113], we will refer to the parameter τ_{K} as to the Keldysh time.

The Keldysh parameter γ_{K} plays a fundamental role in laser-driven ionization dynamics, defining the borderline between weak- and strong-field regimes in laser–matter interactions and providing a quantitative measure for the adiabaticity of photoionization. In the limit of large Keldysh parameters, $\gamma \gg 1$, the Keldysh theory of photoionization yields closed-form equations for the photoionization rate, which recover the well-known weak-field perturbation-theory results for multiphoton ionization. In the opposite limit of $\gamma \ll 1$, the Keldysh formula for the photoionization rate recovers the signature exponential typical of quantum tunneling. In the low-frequency limit, this equation is reduced to the celebrated result for the rate of electron tunneling through a finite potential barrier representing the joint effect of the ion-core potential and the external field.

As one important finding, Eqn (48) relates ΔH_0 to γ_{K}, thus revealing the role of the Keldysh parameter, as well as the pertinent Keldysh time, as a measure of the field-cycle-averaged electron energy variance in the ground state of a hydrogenlike atom in the presence of a laser field.

In a general case of an ultrashort field waveform (44), the equation for $\Phi(t)$ can be conveniently rewritten as

$$\Phi(t) = \frac{1}{\tau_{\mathrm{K}}}\int_{-\infty}^{t} f(\vartheta)\left|\sin\left(\omega\vartheta + \varphi_0\right)\right| \mathrm{d}\vartheta\,. \tag{51}$$

Introducing the dimensionless time $\eta = t/\tau_{\mathrm{K}}$, we find

$$\Phi(\eta) = \int_{-\infty}^{\eta} f(\eta')\left|\sin\left(\gamma_{\mathrm{K}}\eta' + \varphi_0\right)\right| \mathrm{d}\eta'\,. \tag{52}$$

The Keldysh parameter τ_{K} thus sets a natural time scale of quantum evolution in the presence of an external field. Moreover, in its capacity as the measure of the energy variance, the Keldysh parameter, as can be seen from Eqns (48), (50), and (52), is in charge of the evolution rate of such a system.

In the weak-field limit, $\gamma_{\mathrm{K}} \gg 1$, integration in Eqn (52) for a pulse with $\tau_0 \gg T_0$ leads to

$$\Phi(t) \approx \frac{2}{\pi}\,\frac{t}{\tau_{\mathrm{K}}}\,f(t)\,. \tag{53}$$

In this limit, the phase $\Phi(t)$ is a gradually growing function of time (the dashed line in Fig. 5a). The functions $q_+(\eta)$ and $q_-(\eta)$ define the maximum evolution rate of the system whose initial state is ψ_0 and the maximum population rate of the state ket orthogonal to ψ_0 (the solid and dash–dotted lines in Fig. 5a). These functions saturate their bounds at the moment of time τ_1 found from $\Phi(\tau_1) = \pi/2$. Solving this equation for τ_1 near the maximum of the pulse envelope with an assumption that the field variation within the time τ_1 is negligible, i.e., $f(t) \approx 1$, we find

$$\tau_1 \approx \frac{\pi^2}{4}\,\tau_{\mathrm{K}}\,. \tag{54}$$

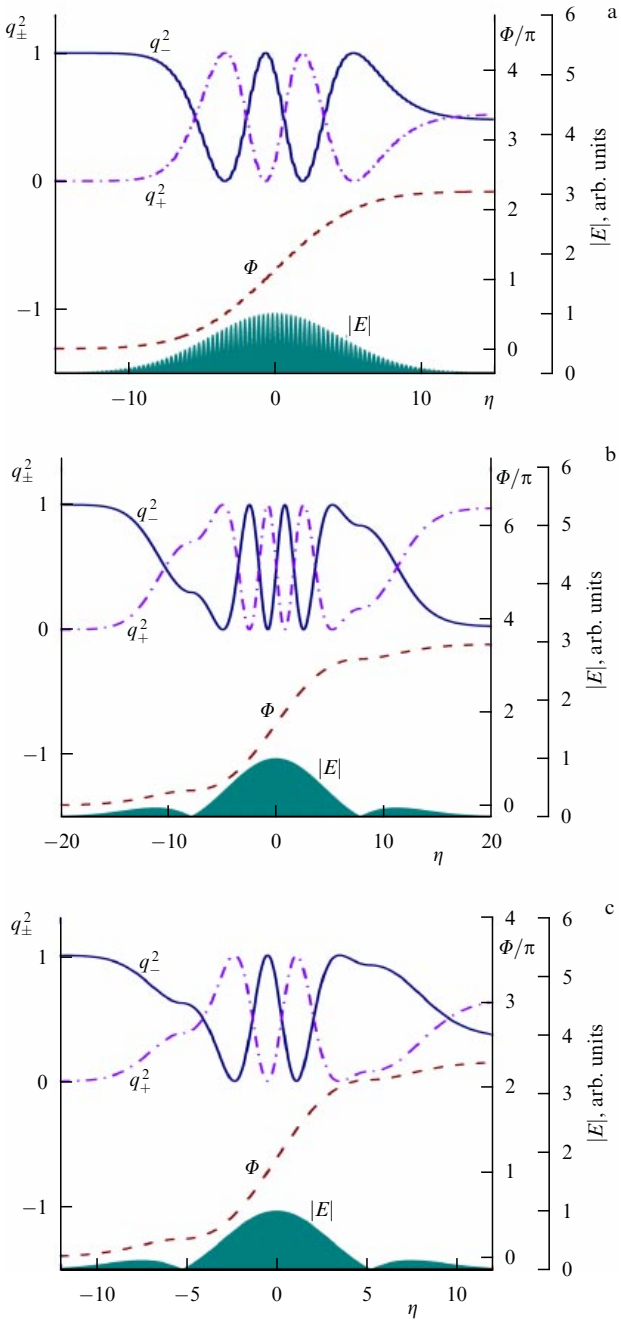

Figure 5. (Color online.) The phase $\Phi(\eta)$ (dashed line) and the functions $q_+^2(\eta)$ (dash–dotted line) and $q_-^2(\eta)$ (solid line) for an optical driver field (shading) with a temporal envelope $f(\eta) = \exp\left(-\eta^2/\eta_0^2\right)$, $\eta = t/\tau_{\mathrm{K}}$, $\gamma_{\mathrm{K}} = 10$, $\eta_0 = 10T_0/\tau_{\mathrm{K}}$, and $\varphi_0 = 0$ (a), $\gamma_{\mathrm{K}} = 0.2$, $\eta_0 = 0.6\pi/\gamma_{\mathrm{K}}$, and $\varphi_0 = \pi/2$ (b), and $\gamma_{\mathrm{K}} = 0.3$, $\eta_0 = 0.3T_0/\tau_{\mathrm{K}}$, and $\varphi_0 = \pi/2$ (c).

Combining Eqn (54) with Eqn (48) gives

$$\tau_1 \approx \frac{\pi}{2}\,\frac{\hbar}{\Delta H_0}\,. \tag{55}$$

This result for τ_1 is quite remarkable as it formally recovers the lower bound τ_{MT} in the Mandelstam–Tamm uncertainty relation (see Eqn (21)). Moreover, when rewritten as a suitable inequality, Eqn (54) recovers the Mandelstam–Tamm uncertainty relation. It should be emphasized here that, in contrast to the analysis leading to the Mandelstam–Tamm uncertainty relation, Eqn (55) was derived for the

time-dependent Hamiltonian $\hat{H}_t$, while the energy variance ΔH_0 in Eqn (55) is defined, in accordance with Eqn (47), as the field-cycle-averaged variance of $\hat{H}_t$.

In the opposite limit of a strong laser field, $\gamma_K \ll 1$, the Keldysh time scale τ_K is much shorter than the field cycle T_0. Figure 5b illustrates typical time dependences of the phase $\Phi(\eta)$ and the functions $q_+(\eta)$ and $q_-(\eta)$ in this regime. As can be readily seen from this figure, the phase $\Phi(t)$ displays significant changes in this limit already within T_0. For very short field waveforms, the field intensity at the peak of the central half-cycle ($|\eta| \approx 7.5$ in Fig. 5b and $|\eta| \approx 5$ in Fig. 5c) is much higher than the field intensity outside this field half-cycle. For such field waveforms, the central half-cycle appears as a well-resolved peak against the overall time envelope (Figs 5b, c). Such a behavior of $\Phi(t)$ is readily understood from the viewpoint of Eqns (51) and (52). In contrast to the weak-field regime, where the phase $\Phi(\eta)$ is a gradually growing function of time (Fig. 5a), in the limit of $\gamma_K \ll 1$, this function exhibits sections of a steep, almost stepwise growth near the peaks of the field intensity, followed by off-peak sections where its variations are much less drastic. It should be noted here that, outside the time interval bounded by $T_\pm$, the functions $q_\pm$ are no longer the bounds of $q(t)$. Yet, these functions still offer important insights into the behavior of the phase $\Phi(t)$, including the inherent properties of this phase that manifest themselves in the time dependence of the photoionization current.

For a qualitative understanding of quantum dynamics in this regime, we take into consideration that the most drastic changes in the phase $\Phi(t)$ are confined within short time intervals around the peaks of the driver intensity. Specifically, near the maximum of the driver field, $\vartheta_p = (p + 1/2)\pi/\omega$, where p is an integer, the change in $\Phi(t)$ for $\varphi_0 = 0$ and $f(\vartheta_p) \approx 1$ is given by

$$\Delta\Phi(t) \approx \frac{1}{\tau_K}\int_{\vartheta_p - t}^{\vartheta_p + t} f(\zeta)\left|\sin(\omega\zeta)\right| \mathrm{d}\zeta = \frac{2}{\gamma_K}\sin(\omega t)\,. \qquad (56)$$

Equation $\Delta\Phi(\tau_2) = \pi/2$ then yields

$$\tau_2 = \frac{1}{\omega}\arcsin\left(\frac{\pi}{4}\gamma_K\right) = \frac{1}{\omega}\arcsin\left(\frac{\pi\hbar}{T_0\Delta H_0}\right). \qquad (57)$$

In the limit of $\gamma_K \ll 1$, we have

$$\tau_2 \approx \frac{\pi}{4}\frac{\gamma_K}{\omega} \approx \frac{\hbar}{2\Delta H_0}\,. \qquad (58)$$

The properties of $\Phi(\eta)$ are remarkable in many respects. As can be seen from TDSE simulations (Fig. 6a), the signature stepwise growth typical of $\Phi(\eta)$ in the $\gamma_K \ll 1$ regime is also observed in the time dependence of the tunneling ionization rate for $\gamma_K \ll 1$, as well as in the related photoelectron current [16, 19, 114–117]. Tunneling ionization dominates photoionization in the $\gamma_K \ll 1$ regime. It is in this limit that well-resolved 'steps' of rapid growth show up in $\Phi(\eta)$ (Fig. 5b). In the opposite limit of $\gamma_K \gg 1$, the phase $\Phi(\eta)$ is a smoothly growing function of time (Fig. 5a). The same tendency is observed in the time dependence of the photoionization current [118, 119]. In the regime of multiphoton ionization, whose criterion is also written as $\gamma_K \gg 1$, the time dependence of the photoionization current becomes smooth, closely following the time integral of the driver intensity envelope (Fig. 6b).

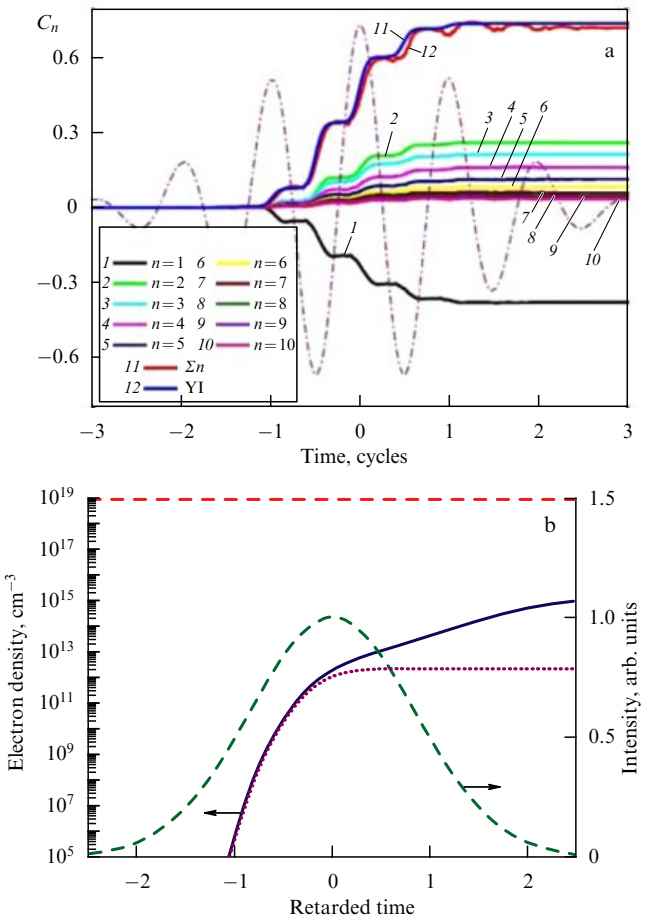

Figure 6. (Color online.) (a) Probabilities of photoionization from quantum states with the principal quantum number n (shown in the figure), calculated by solving the time-dependent Schrödinger equation for a hydrogen atom driven by a laser pulse (dash–dotted line) with a central wavelength of 0.8 μm and a peak intensity of 450 TW cm^{-2}. Also shown is the total photoionization probability Σn (red solid line) and the photoionization probability calculated in the Yudin–Ivanov (YI) approximation [114] (blue solid line). (b) The photoelectron current density in the field of a laser pulse (dashed line) in the regime of multiphoton ionization with (solid line) and without (dotted line) avalanche ionization.

9. The Keldysh parameter and the petahertz limit of optoelectronics

Equations (51)–(58) suggest that the Keldysh parameter γ_K is not only the parameter that defines the borderline between multiphoton and tunneling ionization, but is also the key control of laser-driven quantum dynamics. Since the times τ_1 and τ_2 in Eqns (55) and (58) are defined as the times within which a quantum system evolves from its initial state to a state that is orthogonal, $\Phi(\tau_{1,2}) = \pi/2$, that is, maximally 'dissimilar' to the final state (Figs 4, 7a), we come to realize that, in the $\gamma_K \gg 1$ regime, the Keldysh parameter defines the number of field cycles needed for a system to evolve into an orthogonal state, $M = \tau_1/T_0 = (\pi/8)\gamma_K \gg 1$. Such a view of γ_K is fully consistent with the perturbative treatment of multiphoton ionization [120–124], which helps appreciate multiphoton ionization as a process that spreads out in time, spanning over many field cycles.

In the regime of tunneling ionization, $\gamma_K \ll 1$, the Keldysh parameter defines the ratio of the time it takes for a system to evolve into an orthogonal state to quarter the field cycle, $\tau_2/(T_0/4) = \gamma_K \ll 1$. This inequality indicates a high rate of

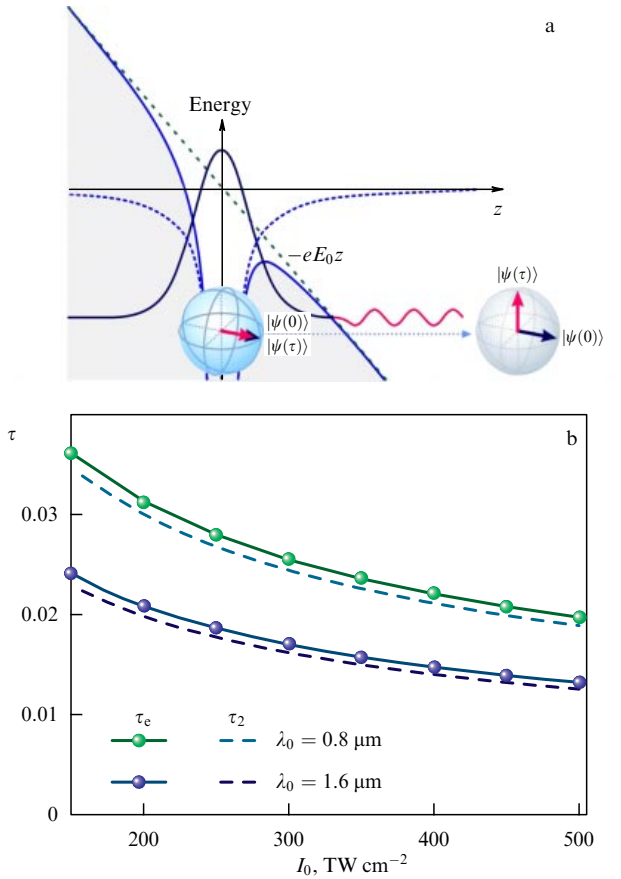

Figure 7. (Color online.) (a) Laser-induced tunneling ionization and the evolution of the state ket $|\psi(t)\rangle$: potential energy without light field (dotted line), the energy of the charge–field dipole interaction (dashed line) and the potential energy at the moment of time corresponding to the peak of the field intensity (solid line). (b) Time τ_2 (dashed lines) and photoionization time τ_e (dots connected by solid lines) in the function of the intensity of laser field with central wavelength of 0.8 μm (green lines) ù 1.6 μm (blue lines).

quantum evolution, such that a quantum system can evolve to a maximally dissimilar state (Fig. 7a) on a time scale as short as $\gamma_K(T_0/4) \ll T_0/4$. For a laser field with a central wavelength of 800 nm and field intensity corresponding to $\gamma_K \approx 0.1$, we find $\tau_2 \approx 0.067$ fs = 67 attoseconds. Viewed as the minimum response time, such a value of τ_2 translates into a speed limit on optical data processing at the level of $w_t \approx 1/\tau_2 \approx 1.5 \times 10^4$ THz = 15 petahertz (PHz). Figure 7b compares the time τ_2 calculated with Eqn (58) with the results of numerical simulations for a typical photoionization time τ_e, defined from the delay time of the pulse of photoelectron current relative to the peak of the laser field intensity. As can be seen from this comparison, Eqn (58) provides an accurate estimate for the typical time scale of photoelectron current buildup — from ≈ 60 to ≈ 100 attoseconds for the range of parameters covered by calculations in Fig. 7b.

Of special interest for advanced information-processing technologies is subfemtosecond photoionization in solids [12, 13, 33, 37, 38]. A detailed understanding of field-cycle-resolved photoionization dynamics in solids is central for achieving the limiting time resolution in attosecond time-resolved studies, shedding light on the fundamental aspects of quantum tunneling, harnessing subfemtosecond dielectric–conductor switching in solids, as well as implementing a high-speed tailoring of optical signals in fiber-optic systems [125–128] and semiconductor waveguide microresonators [129]. As one of the most powerful instigations, research along these lines opens new horizons in high speed electronics, paving the waves toward petahertz optoelectronics [12, 13, 33, 37, 38].

Shown in Fig. 8 are the results of supercomputer simulation [130, 131] of laser-induced reversible ionization in the bulk of diamond. The properties of laser-induced photoelectron current are studied in this simulation by solving the field evolution equation for the laser pulse jointly with the Schrödinger equation for the electron wave function [132]. As an important reference, the red dashed line in Fig. 8 presents the results of the analytical treatment of laser-driven ionization in diamond [133] based on the short-pulse extension of the Keldysh photoionization theory for solids [111, 134]. This treatment is applicable [135] for laser pulses of any pulse width and shape, allowing the photoionization rate to be calculated without averaging over the field cycle, thus providing a powerful tool for the analysis of laser-driven ionization in solids with arbitrary, not necessarily parabolic electron bands. Comparison with supercomputer simulations (cf. the blue solid and red dashed lines in Fig. 8) verifies a high predictive power and accuracy of the analytical treatment of photoionization.

Both supercomputer simulations and analytical modeling suggest that, when the laser driver pulses are sufficiently short, photoelectron current pulses as short as $\tau_c \approx 1.2\tau_2$ can be produced. This regime of laser–matter interaction opens the routes toward high-performance solid-state information processing microcircuits with a speed limit at the level of 10 PHz.

Although the properties of the phase $\Phi(\eta)$ have been found to strongly correlate with the properties of the laser-driven ionization current, the phase $\Phi(\eta)$ is not intended to accurately quantify the rate of laser-driven ionization. Instead, in accordance with its definition (42), this function provides a measure of the fidelity of quantum states $|\psi(0)\rangle$ and $|\psi(t)\rangle$, connecting to the maximum rate of quantum evolution from state $|\psi(0)\rangle$ to state $|\psi(t)\rangle$ (Figs 4, 7). That the function $\Phi(\eta)$, defined as the measure of quantum fidelity, reproduces the key properties of photoionization dynamics suggests a framework whereby universal uncertainty relations can be extended to ultrafast light–matter interactions as a way to reveal and understand the upper bounds on the rates of ultrafast processes involved in such interactions. In this framework, attosecond electron dynamics can be described and understood, as the following section will show, in terms of a suitable information-geometric metric of quantum evolution.

10. Mandelstam–Tamm uncertainty relations and the information-geometric measure of quantum evolution

10.1 Geometry of quantum evolution

When expressed via the angle ϑ and represented in the form of inequality (20), the Mandelstam–Tamm uncertainty relation proves to be especially instructive as it reveals one of the most remarkable properties of this relation and provides the key to the solution of a vast class of problems not only in quantum science and quantum technologies, but also, as we will show below, in thermodynamics. One such remarkable and in many respects unexpected property of the Mandelstam–Tamm uncertainty relation is that its lower bound, $\tau = \tau_{MT}$,

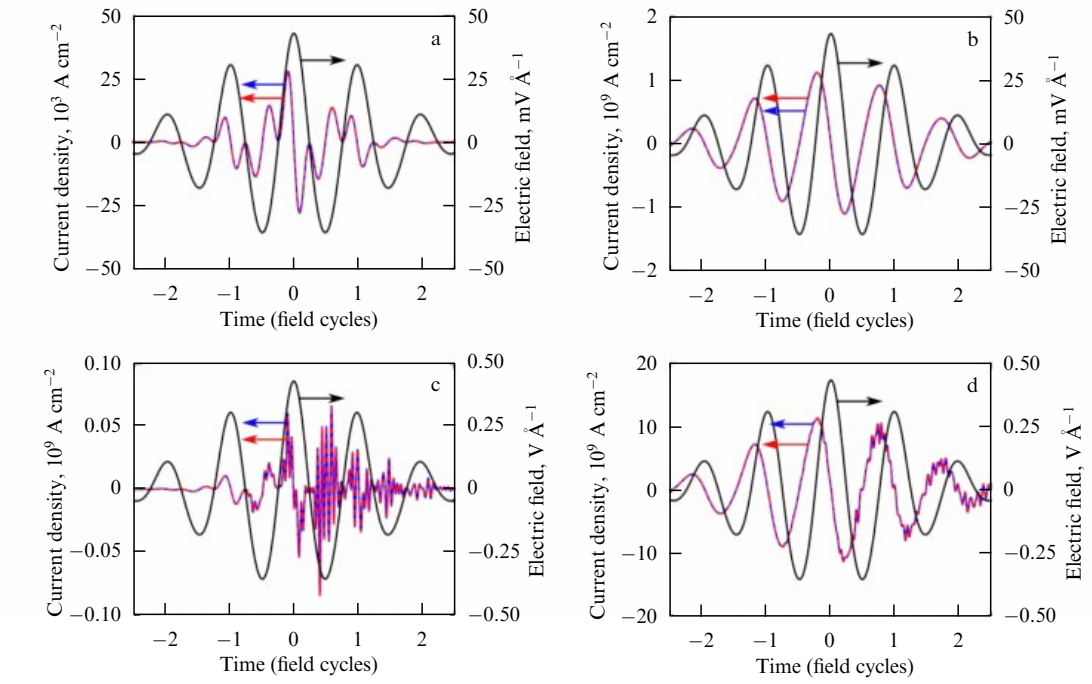

Figure 8. (Color online.) Attosecond dynamics of intraband (a, b) and interband (c, d) currents driven by a laser pulse (black solid line) in bulk diamond. The central wavelength of the laser pulse is 1.6 μm. The peak intensity of the laser field is 0.02 TW cm^{-2} (a, c) and 2.2 TW cm^{-2} (b, d). Also shown are the results of supercomputer simulations (blue line) and calculations performed with the use of the generalized photoionization model [133] (red dashed line).

defining the maximum rate of quantum evolution, is achieved [94, 95, 98, 136] if and only if the system evolves along the geodesic line connecting the states $|\psi(0)\rangle$ and $|\psi(\tau)\rangle$ in the suitable Hilbert space (see Fig. 4).

An angle in a Hilbert space, such as the angle $\vartheta(\psi_0, \psi)$, defined in accordance with Eqn (19), is the only Riemannian metric for a set of rays, e.g., $|\psi(0)\rangle$ and $|\psi(t)\rangle$, that remains invariant with respect to unitary transformations. Such a metric is also in many ways the most natural metric [136]. It is therefore hardly surprising that similar metrics can be found in statistical analysis. Standing out as one of the most important example of such metrics is the metric related to the Fisher information [137–142], defined as the mathematical expectation

$$F(X) = \int p(\xi|X) \left[\frac{\partial \ln p(\xi|X)}{\partial X} \right]^2 \mathrm{d}\xi \tag{59}$$

of an outcome ξ given the condition X with a conditional probability density $p(\xi|X)$.[5] According to the Chentsov theorem [143, 144], the Fisher information metric is the only Riemannian metric that is invariant under sufficient statistics.

10.2 Quantum fidelity and the Fisher information

In the general case, when a pure-state description of a quantum system is impossible or impractical, the angle between the state kets of a quantum system at different instants of time can be defined in terms of the density operator $\hat{\rho}_t = \hat{\rho}(t)$ [92–98, 145–151],

$$\vartheta(\rho_0, \rho_t) = \arccos\left[\sqrt{F_B(\rho_0, \rho_t)}\right], \tag{60}$$

where

$$F_B(t) = F_B(\rho_0, \rho_t) = \left[\mathrm{tr}\left(\sqrt{\rho_0}\,\rho_t\sqrt{\rho_0}\right)^{1/2}\right]^2 \tag{61}$$

is the fidelity of quantum states described by pertinent density matrices.

Introducing a quantum analog of the Fisher information for the estimation of parameter t as [98]

$$F_Q(t) = F_Q(\rho_0, \rho_t) = \mathrm{tr}\left[\hat{\rho}(t)\hat{L}_c^2(t)\right], \tag{62}$$

where $\hat{L}_c(t)$ is the Hermitian operator found as a solution to

$$2\,\frac{\mathrm{d}\hat{\rho}(t)}{\mathrm{d}t} = \hat{\rho}(t)\hat{L}_c(t) + \hat{L}_c(t)\hat{\rho}(t), \tag{63}$$

we arrive at

$$F_B(\rho_t, \rho_{t+\mathrm{d}t}) = 1 - \frac{F_Q(t)}{4}\,(\mathrm{d}t)^2 + O(\mathrm{d}t)^3. \tag{64}$$

As can be seen from Eqn (64), the quantum Fisher information $F_Q(t)$ defines the square of the instantaneous rate at which the distance between close states ρ_t and $\rho_{t+\mathrm{d}t}$ changes at instant t. Given the evolution $\rho(t)$, the path length can thus be found as [98]

$$D_Q = \frac{1}{2}\int_0^\tau \left[F_Q(t)\right]^{1/2} \mathrm{d}t. \tag{65}$$

The distance between ρ_1 and ρ_2, defined by the angle $\vartheta(\rho_1, \rho_2)$, along the geodesic line is always shorter than the path length D_Q as dictated by the actual evolution $\rho(t)$,

$$\vartheta \leqslant \frac{1}{2}\int_0^\tau \left[F_Q(t)\right]^{1/2} \mathrm{d}t. \tag{66}$$

When written in a differential form, Eqn (66) leads to the quantum Cramér–Rao bound, $\delta t \geqslant F_Q^{-1/2}$.

[5] Because the metrics of this class are so natural, they have been known in the early literature even before the seminal work by Fisher (see, e.g., Refs [137, 141]).

10.3 Uncertainty relation and the Cramér–Rao bound

To gain deeper insights into how the energy–time uncertainty relation connects to the quantum Fisher information, it is instructive to examine quantum evolution of pure states governed by a unitary evolution operator $\hat{U}(t)$. Using the definition (62) and solving Eqn (63) for pure states, $[\rho(t)]^2 = \rho(t)$, we find [95, 98]

$$F_Q(t) = \frac{4}{\hbar^2}\left\langle \left[\Delta K(t)\right]^2 \right\rangle , \tag{67}$$

where $\left\langle \left[\Delta K(t)\right]^2 \right\rangle$ is the variance of a Hermitian operator defined as

$$\hat{K}(t) = \frac{\hbar}{\mathrm{i}} \frac{\mathrm{d}\hat{U}^{\dagger}(t)}{\mathrm{d}t}\, \hat{U}(t) . \tag{68}$$

The quantum Cramér–Rao bound, $\delta t \geqslant F_Q^{-1/2}$, then sets the following limit on the error of t estimation:

$$\delta t \geqslant \frac{\hbar}{2\Delta K} . \tag{69}$$

In the general case of a time-dependent Hamiltonian $\hat{H}_t$, $\Delta K \neq \Delta H_t$, the limit of Eqn (69) differs from the lower bound in the Mandelstam–Tamm energy–time uncertainty relation (21). This bound, however, is recovered [95, 98] for stationary Hamiltonians, $\hat{H}_t = \hat{H}$. For such Hamiltonians, $\hat{U}(t) = \exp(-\mathrm{i}\hat{H}t/\hbar)$ and $\hat{K}(t) = \hat{H}$. Setting $\vartheta(\rho_1, \rho_2) = \pi/2$, as necessary to reproduce the Mandelstam–Tamm relation (21), derived with $\langle\psi(0)|\psi(\tau)\rangle = 0$, and applying inequality (69), we arrive at

$$\tau \geqslant \frac{\pi}{2}\frac{\hbar}{\Delta H_0} , \tag{70}$$

where ΔH_0 is the variance of the stationary Hamiltonian $\hat{H}$ with respect to the initial state ψ_0.

Inequality (70) recovers the Mandelstam–Tamm uncertainty relation (21) and saturates simultaneously with the quantum Cramér–Rao bound.

11. Nonquantum nature of the quantum speed limit

Until recently, the quantum speed limit dictated by the Mandelstam–Tamm uncertainty relation has been viewed as a purely quantum phenomenon that has no classical analog. Indeed, analysis presented in the original work by Mandelstam and Tamm is based on quantum evolution equations and involves quantum-mechanical averaging, yielding inequalities for quantum-mechanical expectation values. That the Mandelstam–Tamm energy–time uncertainty vanishes in the $\hbar \to 0$ limit is broadly interpreted as a manifestation of the quantum nature of the speed limit as defined by Eqns (26) and (27).

The latest studies, however, suggest [152, 153] that this view of the τ_{QSL} speed limit should be revised. The Mandelstam–Tamm energy–time uncertainty relations prove to be applicable to a much broader class of systems, remaining valid even beyond the realm of quantum mechanics. The 'quantum speed limit' turns out to be nonquantum.

To understand whether the quantum nature of a system and its dynamics is indeed necessary and significant for the existence of the limit (26), it is instructive to resort to Eqn (10) as the key point in the derivation of the Mandelstam–Tamm energy–time uncertainty relation. The evolution of the operator $\hat{R}$ in this equation owes its quantumness to the commutator $[\hat{H}, \hat{R}]$, chosen in such a way as to obey the general quantization rule. When written in a matrix form, Eqn (10) leads to the Liouville–von Neumann equation for the density operator $\rho(\mathbf{r}, t)$,

$$\mathrm{i}\,\frac{\partial\rho(\mathbf{r}, t)}{\partial t} = \hat{L}\rho(\mathbf{r}, t) , \tag{71}$$

where $\hat{L}$ is the Liouville operator. For quantum systems, this operator is defined in such a way as to postulate a suitable quantization rule,

$$\hat{L}\hat{\rho}(\mathbf{r}, t) = \hbar^{-1}\left[\hat{H}, \rho(\mathbf{r}, t)\right] . \tag{72}$$

However, the domain of validity of Eqn (71) is in no way limited to quantum mechanics. This equation is satisfied for a vast class of physical — not necessarily mechanical — systems allowing description in the framework of the Hamiltonian formalism. Examples of such systems are widely known in optics [154–160] and statistical physics [161, 162]. In classical mechanics, the Liouville equation is formulated for a probability distribution $\rho(\mathbf{r}, t)$ in an N-dimensional phase space spanned by generalized coordinates q_j and canonically conjugate momenta p_j, $\mathbf{r} = (x_1, \ldots, x_N; p_1, \ldots, p_N)$. The Liouville operator in this setting is defined via the Poisson bracket,

$$\mathrm{i}\hat{L}\rho(\mathbf{r}, t) = \sum_{j=1}^{N}\left(\frac{\partial H}{\partial p_j}\frac{\partial\rho}{\partial q_j} - \frac{\partial H}{\partial q_j}\frac{\partial\rho}{\partial p_j}\right) , \tag{73}$$

where $H(\mathbf{r})$ is the Hamilton function.

As can be seen from Eqns (10) and (71)–(73), it is the specific choice of the bracket operator rather than the general properties of the solutions of the Liouville–von Neumann equation that makes τ_{MT} vanish in the limit of $\hbar \to 0$, $\tau_{\mathrm{MT}} \to 0$. That the form of the bracket operator defines the granularity of the phase space is well known in signal analysis [163–165]. Instructive examples of such granularity are readily found in Hamiltonian optics. Liouville-equation analysis of systems of this type is fully analogous to the description of quantum evolution. Specifically, the diffraction limit of spatial resolution can be viewed as an optical analog of quantum uncertainty as dictated by the general form of the evolution equation. Formally, the diffraction limit is recovered by replacing $\hbar$ in quantum uncertainty relations with $\lambda/2\pi$, λ being the radiation wavelength. The limiting transition $\lambda \to \infty$ then gives $\tau_{\mathrm{MT}} \to 0$ and corresponds to ray-optic approximation [155, 156, 166]. Position–momentum uncertainty relations have the same form in optics and quantum mechanics, $\Delta x \Delta p_x \geqslant \kappa/2$. Their physical content is, however, different. In quantum mechanics, $\kappa = \hbar$, this inequality is known as the Heisenberg uncertainty relation. In optics, $\kappa = \lambda/2\pi$, this inequality expresses the diffraction limit [155, 156].

As shown by Okuyama and Ohzeki [153], the overlap factors $\vartheta(t) = \langle\rho^{\alpha}|\rho^{\alpha}(t)\rangle$, defined for a distribution function $\rho(t)$ with $\rho^{\alpha} = \rho^{\alpha}(0)$, meet the relation

$$\tau \geqslant \tau_{\mathrm{CSL}}^{(\alpha)} = \left[\frac{\vartheta(0)}{\langle\rho^{\alpha}|\hat{L}^2|\rho^{\alpha}\rangle}\right]^{1/2} \arccos\left[\frac{\vartheta(\tau)}{\vartheta(0)}\right] \tag{74}$$

for any real α.

Thus, similar to the evolution rate of a quantum system, the evolution rate of a classical system is bounded from above. Inequality (74) sets an upper bound for this rate, providing a classical analog of the energy–time uncertainty relation.

12. Thermodynamic uncertainty limit

12.1 Information metric and thermodynamic uncertainties

The ray-geometric view of state-ket evolution in the statistics space discussed in Section 10 provides a framework that enables a unified description of the dynamics of a quantum system and a thermodynamic ensemble. In this framework, fluctuations in a thermodynamic system obey relations similar to the quantum uncertainty relations [167–171]. These relations reveal fundamental thermodynamic limitations on the performance of complex biomolecular and microbiological systems [172–178], such as molecular motors and pumps [179, 180], Brownian biological clocks [181–183], membrane proteins [184–189], as well as distributed neural networks involved in complex brain functions, such as information processing and memory formation [190–194]. COVID-19-related research of the past few months provides a unique material that enables a detailed thermodynamic analysis of the affinity of spike proteins of SARS-CoV and SARS-CoV-2 coronaviruses whereby these viruses recognize receptor enzymes and hijack the biomolecular machinery of a host cell [200, 201].

To understand the information-statistical content of thermodynamic uncertainty relations, it is instructive to resort to Eqn (59) and examine the Fisher information $F(\zeta)$ for the estimation of a thermodynamic parameter ζ. The energy variance due to fluctuations of ζ can be expressed through this Fisher information as [167]

$$F(\zeta) = \beta^2 \left\langle \left(\left\langle \frac{\partial E}{\partial \zeta} \right\rangle - \frac{\partial E}{\partial \zeta} \right)^2 \right\rangle , \tag{75}$$

where $\beta = 1/(k_{\rm B}T)$, T is the temperature, and $k_{\rm B}$ is the Boltzmann constant.

Choosing the inverse temperature as the control thermodynamic parameter, $\zeta = \beta$, we find from Eqn (75)

$$F(\beta) = \left\langle \left(\langle E \rangle - E \right)^2 \right\rangle . \tag{76}$$

Applying the inequality for the Cramér–Rao bound [202, 203],

$$\left\langle (\bar{\beta} - \beta)^2 \right\rangle \geqslant \frac{1}{F(\beta)} , \tag{77}$$

we arrive at

$$\Delta E \Delta \beta \geqslant 1 , \tag{78}$$

where, by definition, $(\Delta\beta)^2 = \langle (\bar{\beta} - \beta)^2 \rangle$.

Eqn (78) can be represented as

$$\Delta E \Delta \left(\frac{1}{T} \right) \geqslant k_{\rm B} . \tag{79}$$

Defining the Fisher information as a function of other variables and using the inequalities for the pertinent Cramér–Rao bounds, we can derive similar uncertainty relations for other thermodynamic parameters. Specifically, when applied to the fluctuations of the entropy, the volume, and the number of particles, this procedure leads to [168–171]

$$\Delta S \Delta T \geqslant k_{\rm B} T , \tag{80}$$

$$\Delta V \Delta P \geqslant k_{\rm B} T , \tag{81}$$

$$\Delta N \Delta \mu \geqslant k_{\rm B} T , \tag{82}$$

where P is the pressure and μ is the chemical potential.

12.2 The thermodynamic limit for the temperature threshold of membrane proteins

Uncertainty relations for thermodynamic parameters (Eqns (78)–(82)) shed light on the fundamental physical and chemical properties of complex biological systems. As an important example, we consider a thermodynamic model of thermosensitive ion channels in cellular membranes. Ion channels of this type (TRP channels) can respond to temperature variations by switching between closed- and open-gate states, controlling via such gating the density of ions on different sides of a membrane, thus inducing an electric potential [184–189, 204–214]. Advanced biotechnologies [215–221] enable a genetic encoding of the expression of thermosensitive membrane channels in cells of a certain type or even in certain intracellular compartments [204, 208–214, 222–227], targeted via a suitable virus vector delivery. The cells that express the thermosensitive channels can be controlled with local changes in temperature.

As their key property, thermosensitive membrane channels can respond to small temperature variations in the intercellular space. Within the framework of a two-state thermodynamic model, this property of thermosensitive channels is described [186–189] in terms of the probability of channel switching between the open- and closed-gate states:

$$p_g = \frac{1}{1 + \exp\left(-\Delta S_g/R\right) \exp\left[\Delta H_g/(RT)\right]} , \tag{83}$$

where R is the universal gas constant and ΔH_g and ΔS_g are the enthalpy and entropy changes related to channel gating.

Within a temperature range where $|\Delta H_g|/(RT) \gg 1$ and $|\Delta H_g| \gg T|\Delta S_g|$, Eqn (83) can be approximated as

$$p_g \approx \exp\left(-\beta N_{\rm A} \Delta H_g\right) ,$$

where $N_{\rm A}$ is the Avogadro number. Within this temperature range, the probability of channel gating is exponentially small (Fig. 9) — most of the channels remain closed. In the opposite limit, when $|\Delta H_g|/(RT) \ll 1$ and $|\Delta H_g| \ll T|\Delta S_g|$, the probability of channel gating saturates, tending to a constant determined by the entropy change $|\Delta S|$ (see Fig. 9). Finally, near the temperature $T_{\rm c} = |\Delta H_g/\Delta S_g|$, the probability of channel gating is a rapidly growing function of temperature. Expanding the channel gating probability as a power series in $\delta T = T - T_{\rm c}$ about $T_{\rm c}$, we find

$$p_g \approx \frac{1}{2} \left(1 + \frac{\delta T}{2\Delta T_0} \right) , \tag{84}$$

where

$$\Delta T_0 = \frac{R T_{\rm c}^2}{\Delta H_g} . \tag{85}$$

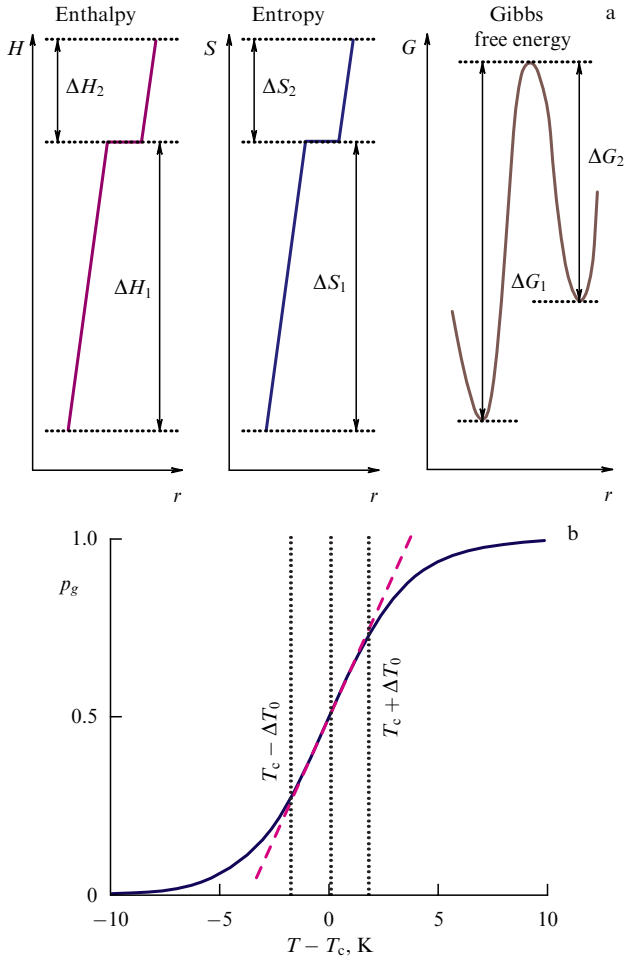

Figure 9. (Color online.) (a) Thermodynamic model of thermosensitive ion channel gating with enthalpy change $\Delta H_g = \Delta H_1 + \Delta H_2$, entropy change $\Delta S_g = \Delta S_1 + \Delta S_2$, and Gibbs free energy change $\Delta G = \Delta H_g - T\Delta S_g = \Delta G_1 - \Delta G_2$ shown as functions of the generalized reaction coordinate r. (b) The gating probability of a thermal channel as a function of temperature for $\Delta H_g = 100$ kcal mol^{-1} and $\Delta S_g = 330$ cal (mol K)$^{-1}$. The vertical dotted lines show the temperature $T = T_c$ and the temperature range $T = T_c \pm \Delta T_0$.

As can be seen from Eqns (84) and (85), the channels are gated within a small interval of temperatures $T_c \pm \Delta T_0$ near the critical point T_c (shown by the vertical dotted lines in Fig. 9b). The width of this interval controls the temperature sensitivity of the channel. For a gating enthalpy of $\Delta H_g \approx 100$ kcal mol^{-1}, typical of TRPV channels [186, 187] with $T_c \approx 300$ K, we find $\Delta T_0 \approx 1.8$ K. A group of a few thermosensitive channels can thus provide a temperature sensitivity at the level of 0.1 K.

To gain deeper insights into this result, it is instructive to represent Eqn (85) in a form analogous to the energy–time uncertainty relation:

$$\Delta T \geqslant \Delta T_0 = \frac{RT_c^2}{\Delta H_g} \,. \tag{86}$$

As can be seen from Eqn (86), the enthalpy change ΔH_g plays the role of the key parameter controlling the sensitivity of the channel to temperature variations. The role of ΔH_g in thermosensitive channel gating is thus similar to the role of energy variance in quantum dynamics.

13. Conclusion

Rapidly progressing optical physics and laser technologies provide a unique toolbox for time-resolved studies of ultrafast phenomena, offering means to detect extraordinarily brief transient events on a time scale of tens of attoseconds. However, the most difficult questions related to the physical content and interpretation of such measurements remain open, reflecting the fundamental difficulties in the definition of time encountered in quantum mechanics. En route toward resolving this difficulty, we are led to extend universal uncertainty relations to ultrafast light–matter interactions. Such a generalized uncertainty sets a lower bound on the response time inherent in attosecond electronic dynamics driven by ultrashort laser pulses, revealing a fundamental limitation on the performance of the next-generation photonic information systems — systems of petahertz optoelectronics. The ray-geometric view of state-ket evolution in the statistics space provides a framework that enables a unified description of the dynamics of a quantum system and a thermodynamic ensemble. Within this framework, attosecond electron dynamics can be described and understood in terms of a universal information-geometric metric of quantum evolution. The quest for the time lost in quantum mechanics leads to a realization of fundamental thermodynamic limitations on the performance of complex biomolecular and microbiological systems, as well as distributed neural networks involved in complex brain functions, including information processing and memory formation.

Acknowledgments

I am deeply grateful to K V Anokhin, A Baltuška, V V Belousov, A A Voronin, A A Lanin, V Ya Panchenko, E E Serebryannikov, M O Scully, A B Fedotov, and I V Fedotov for numerous stimulating discussions and long-standing fruitful collaboration.

This review was written with a support from the Russian Foundation for Basic Research (project no. 19-12-50162). Original research reviewed in this work was supported in part by the Russian Foundation for Basic Research (project nos. 18-29-20031 and 19-02-00473), Ministry of Science and Higher Education of the Russian Federation (project 14.Z50.31.0040, February 17, 2017), and the Welch Foundation (grant A-1801-20180324). Research into ultrabroadband nonlinear optics was supported by the Russian Science Foundation (project no. 20-12-00088). Research into neurothermodynamics was supported in part by the "Brain, cognitive systems, and artificial intelligence" interdisciplinary scientific school at Lomonosov Moscow State University.

References

1. Corkum P B, Krausz F *Nat. Phys.* **3** 381 (2007)
2. Baltuška A et al. *Nature* **421** 611 (2003)
3. Goulielmakis E et al. *Science* **305** 1267 (2004)
4. Kienberger R et al. *Nature* **427** 817 (2004)
5. Goulielmakis E et al. *Nature* **466** 739 (2010)
6. Krausz F, Ivanov M *Rev. Mod. Phys.* **81** 163 (2009)
7. Reiter F et al. *Phys. Rev. Lett.* **105** 243902 (2010)
8. Goulielmakis E et al. *Science* **320** 1614 (2008)
9. Zheltikov A M *Phys. Usp.* **54** 29 (2011); *Usp. Fiz. Nauk* **181** 33 (2011)
10. Hassan M Th et al. *Nature* **530** 66 (2016)
11. Cavalieri A L et al. *Nature* **449** 1029 (2007)
12. Schiffrin A et al. *Nature* **493** 70 (2013)
13. Schultze M et al. *Nature* **493** 75 (2013)

14. Schubert O et al. *Nat. Photon.* **8** 119 (2014)
15. Hohenleutner M et al. *Nature* **523** 572 (2015)
16. Uiberacker M et al. *Nature* **446** 627 (2007)
17. Pfeiffer A N et al. *Nat. Phys.* **8** 76 (2012)
18. Ghimire S et al. *Nat. Phys.* **7** 138 (2011)
19. Mitrofanov A V et al. *Phys. Rev. Lett.* **106** 147401 (2011)
20. Vampa G et al. *Nature* **522** 462 (2015)
21. Vampa G et al. *Phys. Rev. Lett.* **115** 193603 (2015)
22. Luu T T et al. *Nature* **521** 498 (2015)
23. Lanin A A, Stepanov E A, Fedotov A B, Zheltikov A M *Optica* **4** 516 (2017)
24. Langer F et al. *Nature* **533** 225 (2016)
25. You Y S, Reis D A, Ghimire S *Nat. Phys.* **13** 345 (2017)
26. Rybka T et al. *Nat. Photon.* **10** 667 (2016)
27. Higuchi T et al. *Nature* **550** 224 (2017)
28. Langer F et al. *Nat. Photon.* **11** 227 (2017)
29. Schultze M et al. *Science* **346** 1348 (2014)
30. Lucchini M et al. *Science* **353** 916 (2016)
31. Schlaepfer F et al. *Nat. Phys.* **14** 560 (2018)
32. Vampa G et al. *Nat. Photon.* **12** 465 (2018)
33. Sommer A et al. *Nature* **534** 86 (2016)
34. Langer F et al. *Nature* **557** 76 (2018)
35. Lanin A A et al. *Opt. Lett.* **44** 1888 (2019)
36. Pupeza I et al. *Nature* **577** 52 (2020)
37. Krausz F, Stockman M I *Nat. Photon.* **8** 205 (2014)
38. Garg M et al. *Nature* **538** 359 (2016)
39. Zheltikov A M *JETP Lett.* **90** 90 (2009); *Pis'ma Zh. Eksp. Teor. Fiz.* **90** 98 (2009)
40. Zheltikov A M *Phys. Usp.* **60** 1087 (2017); *Usp. Fiz. Nauk* **187** 1169 (2017)
41. Akagi H et al. *Science* **325** 1364 (2009)
42. Schultze M et al. *Science* **328** 1658 (2010)
43. Mauritsson J et al. *Phys. Rev. Lett.* **105** 053001 (2010)
44. Eckle P et al. *Science* **322** 1525 (2008)
45. Verhoef A J et al. *Phys. Rev. Lett.* **104** 163904 (2010)
46. Pfeiffer A N et al. *Nat. Phys.* **8** 76 (2012)
47. Zheltikov A M et al. *Phys. Rev. Lett.* **103** 033901 (2009)
48. Reiter F et al. *Phys. Rev. Lett.* **105** 243902 (2010)
49. Zheltikov A M et al. *Phys. Rev. Lett.* **105** 103901 (2010)
50. MacColl L A *Phys. Rev.* **40** 621 (1932)
51. Hauge E H, Støvneng J A *Rev. Mod. Phys.* **61** 917 (1989)
52. Landauer R, Martin Th *Rev. Mod. Phys.* **66** 217 (1994)
53. Landsman A S, Keller U *Phys. Rep.* **547** 1 (2015)
54. Sokolovski D, Connor J N L *Phys. Rev. A* **42** 6512 (1990)
55. Sokolovski D, Connor J N L *Phys. Rev. A* **44** 1500 (1991)
56. Sokolovski D, Connor J N L *Phys. Rev. A* **47** 4677 (1993)
57. Sokolovski D *Phys. Rev. Lett.* **25** 4946 (1997)
58. Sokolovski D *Phys. Rev. A* **59** 1003 (1999)
59. de Carvalho C A A, Nussenzveig H M *Phys. Rep.* **364** 83 (2002)
60. Sokolovski D, Akhmatskaya E *Commun. Phys.* **1** 47 (2018)
61. Landau L, Teller E *Phys. Z. Sowjetunion* **10** 34 (1936); Landau L D, Teller E, in Landau L D *Izbrannye Trudy* (Selected Works) Vol. 1 (Moscow: Nauka, 1969) p. 181, paper 21
62. Nikitin E E, Pitaevskii L P *Phys. Usp.* **36** 851 (1993); *Usp. Fiz. Nauk* **163** (9) 101 (1993)
63. Popov V S *Phys. Usp.* **47** 855 (2004); *Usp. Fiz. Nauk* **174** 921 (2004)
64. Fulling S A *Phys. Rev. D* **7** 2850 (1973)
65. Unruh W G *Phys. Rev. D* **14** 870 (1976)
66. Hawking S W *Nature* **248** 30 (1974)
67. Hartle J B, Hawking S W *Phys. Rev. D* **13** 2188 (1976)
68. Busch P *Found. Phys.* **20** 1 (1990)
69. Muga J G, Mayato R S, Egusquiza Í L (Eds) *Time in Quantum Mechanics* Vol. 1 (Lecture Notes in Physics, Vol. 734) (Heidelberg: Springer, 2008)
70. Bohr N *Phil. Mag. 6* **26** 1 (1913)
71. Bohr N *Phil. Mag. 6* **26** 476 (1913)
72. Bohr N *Phil. Mag. 6* **26** 857 (1913)
73. Beller M *Quantum Dialogue: the Making of a Revolution* (Chicago, IL: Univ. of Chicago Press, 1999)
74. Heisenberg W *Z. Phys.* **43** 172 (1927)
75. Bohr N *Nature* **121** 580 (1928)
76. Pauli W, in *Handbuch der Physik* Vol. 24 (Eds H Geiger, K Scheel) (Berlin: Springer, 1933) p. 83
77. Wigner E P *Rev. Mod. Phys.* **29** 255 (1957)
78. Galapon E A, Caballar R F, Bahague R T (Jr.) *Phys. Rev. Lett.* **93** 180406 (2004)
79. Peres A *Am. J. Phys.* **48** 552 (1980)
80. Eisenbud L "The formal properties of nuclear collisions", Ph.D. Dissertation (Princeton, NJ: Princeton Univ., 1948)
81. Bohm D *Quantum Theory* (New York: Prentice-Hall, 1951)
82. Wigner E P *Phys. Rev.* **98** 145 (1955)
83. Smith F T *Phys. Rev.* **118** 349 (1960)
84. Serebryannikov E E, Zheltikov A M *Optica* **3** 1201 (2016)
85. Corkum P B *Phys. Rev. Lett.* **71** 1994 (1993); Corkum P *Herald Russ. Akad. Sci.* **86** 426 (2016); *Vestn. Ross. Akad. Nauk* **86** 1073 (2016)
86. Lewenstein M et al. *Phys. Rev. A* **49** 2117 (1994)
87. Serebryannikov E E, Zheltikov A M *Phys. Rev. Lett.* **116** 123901 (2016)
88. Mandelstam L I, Tamm I E *Izv. Akad. Nauk SSSR Ser. Fiz.* **9** 122 (1945); Mandelstam L, Tamm I *J. Phys. USSR* **9** 249 (1945)
89. Bohr N "Discussion with Einstein on epistemological problems in atomic physics", in *Albert Einstein: Philosopher – Scientist* (Ed. P A Schilpp) (Evanston, IL: Library of Living Philosophers, 1949) p. 201
90. Holevo A S *Probabilistic and Statistical Aspects of Quantum Theory* (Amsterdam: North-Holland, 1982); Translated from Russian: *Veroyatnostnye i Statisticheskie Aspekty Kvantovoi Teorii* (Moscow: Nauka, 1980)
91. Hilgevoord J *Am. J. Phys.* **66** 396 (1998)
92. Anandan J, Aharonov Y *Phys. Rev. Lett.* **65** 1697 (1990)
93. Deffner S, Lutz E *J. Phys. A* **46** 335302 (2013)
94. Braunstein S L, Caves C M *Phys. Rev. Lett.* **72** 3439 (1994)
95. Caves C M, Drummond P D *Rev. Mod. Phys.* **66** 481 (1994)
96. Lloyd S *Nature* **406** 1047 (2000)
97. Giovannetti V, Lloyd S, Maccone L *Nat. Photon.* **5** 222 (2011)
98. Taddei M M et al. *Phys. Rev. Lett.* **110** 050402 (2013)
99. del Campo A et al. *Phys. Rev. Lett.* **110** 050403 (2013)
100. Lewis-Swan R J et al. *Nat. Rev. Phys.* **1** 627 (2019)
101. Deffner S *Phys. Rev. Res.* **2** 013161 (2020)
102. Caneva T et al. *Phys. Rev. Lett.* **103** 240501 (2009)
103. Okuyama M, Ohzeki M *J. Phys. A* **51** 318001 (2018)
104. Magnus W *Commun. Pure Appl. Math.* **7** 649 (1954)
105. Zheltikov A M *Phys. Rev. A* **94** 043412 (2016)
106. Zheltikov A M *J. Phys. B* **50** 092001 (2017)
107. Zheltikov A *J. Opt. Soc. Am. B* **36** A168 (2019)
108. Pfeifer P *Phys. Rev. Lett.* **70** 3365 (1993)
109. Zheltikov A M *Opt. Lett.* **46** 989 (2021)
110. Pfeifer P, Fröhlich J *Rev. Mod. Phys.* **67** 759 (1995)
111. Keldysh L V *Sov. Phys. JETP* **20** 1307 (1965); *Zh. Eksp. Teor. Fiz.* **47** 1945 (1964)
112. Orlando G et al. *J. Phys. B* **47** 204002 (2014)
113. Orlando G et al. *Phys. Rev. A* **89** 014102 (2014)
114. Yudin G L, Ivanov M Yu *Phys. Rev. A* **64** 013409 (2001)
115. Serebryannikov E E, Zheltikov A M *Phys. Rev. Lett.* **113** 043901 (2014)
116. Serebryannikov E E et al. *Phys. Rev. A* **80** 053809 (2009)
117. Fuji T, Suzuki T, Serebryannikov E E, Zheltikov A *Phys. Rev. A* **80** 063822 (2009)
118. Goulielmakis E et al. *Opt. Lett.* **33** 1407 (2008)
119. Serebryannikov E E, Goulielmakis E, Zheltikov A M *New J. Phys.* **10** 093001 (2008)
120. Delone N B *Sov. Phys. Usp.* **18** 169 (1975); *Usp. Fiz. Nauk* **115** 361 (1975)
121. Delone N B *Usp. Fiz. Nauk* **148** 551 (1986)
122. Perelomov A M, Popov V S, Terent'ev M V *Sov. Phys. JETP* **23** 924 (1966); *Zh. Eksp. Teor. Fiz.* **50** 1393 (1966); Karnakov B M, Mur V D, Popruzhenko S V, Popov V S *Phys. Usp.* **58** 3 (2015); *Usp. Fiz. Nauk* **185** 3 (2015)
123. Zheltikov A M, Koroteev N I *Phys. Usp.* **42** 321 (1999); *Usp. Fiz. Nauk* **169** 385 (1999)
124. Zheltikov A M *Phys. Usp.* **49** 605 (2006); *Usp. Fiz. Nauk* **176** 623 (2006)
125. Serebryannikov E E, Zheltikov A M *Phys. Rev. A* **76** 013820 (2007)
126. Fedotov A B, Serebryannikov E E, Zheltikov A M *Phys. Rev. A* **76** 053811 (2007)

127. Voronin A A, Zheltikov A M *Phys. Rev. A* **94** 023824 (2016)
128. Voronin A A, Zheltikov A M *Sci. Rep.* **10** 12253 (2020)
129. Savvin A D et al. *Opt. Commun.* **284** 1652 (2011)
130. Zhokhov P A, Zheltikov A M *Sci. Rep.* **8** 1824 (2018)
131. Voronin A A, Zheltikov A M *Phys. Usp.* **59** 869 (2016); *Usp. Fiz. Nauk* **186** 957 (2016)
132. Zhokhov P A, Zheltikov A M *Phys. Rev. A* **96** 033415 (2017)
133. Zhokhov P, Zheltikov A M *Phys. Rev. Lett.* **113** 133903 (2014)
134. Keldysh L V *Phys. Usp.* **60** 1187 (2017); *Usp. Fiz. Nauk* **187** 1280 (2017); *Herald Russ. Acad. Sci.* **86** 413 (2016); *Vestn. Ross. Akad. Nauk* **86** 1059 (2016)
135. Voronin A A, Zheltikov A M *Sci. Rep.* **7** 36263 (2017)
136. Wootters W K *Phys. Rev. D* **23** 357 (1981)
137. Edgeworth F Y *J. R. Stat. Soc.* **71** 381 (1908)
138. Fisher R A *Proc. R. Soc. Edinburgh* **42** 321 (1922)
139. Fisher R A *Proc. Camb. Philos. Soc.* **22** 700 (1925)
140. Fisher R A *Statistical Methods for Research Workers* (Edinburgh: Oliver and Boyd, 1925)
141. Stigler S M *The History of Statistics*: *the Measurements of Uncertainty before 1900* (Cambridge, MA: Belknap Press of Harvard Univ. Press, 1986)
142. Schervish M J *Theory of Statistics* (New York: Springer-Verlag, 1995)
143. Chentsov N N *Math. Operationsforsch. Stat.* **9** 267 (1978)
144. Friedlander F G, Joshi M *Introduction to the Theory of Distributions* 2nd ed. (Cambridge, UK: Cambridge Univ. Press, 1998)
145. Uhlmann A *Phys. Lett. A* **161** 329 (1992)
146. Margolus N, Levitin L B *Physica D* **120** 188 (1998)
147. Levitin L B, Toffoli T *Phys. Rev. Lett.* **103** 160502 (2009)
148. Jones P J, Kok P *Phys. Rev. A* **82** 022107 (2010)
149. Boixo S et al. *Phys. Rev. Lett.* **98** 090401 (2007)
150. Escher B M et al. *Phys. Rev. Lett.* **109** 190404 (2012)
151. Escher B M, de Matos Filho R L, Davidovich L *Nat. Phys.* **7** 406 (2011)
152. Shanahan B et al. *Phys. Rev. Lett.* **120** 070401 (2018)
153. Okuyama M, Ohzeki M *Phys. Rev. Lett.* **120** 070402 (2018)
154. Eve M *Proc. R. Soc. Lond. A* **347** 405 (1976)
155. Stoler D *J. Opt. Soc. Am.* **71** 334 (1981)
156. Marcuse D *Light Transmission Optics* (Amsterdam: Van Nostrand Reinhold, 1972)
157. Snyder A W, Love J D *Optical Waveguide Theory* (London: Chapman and Hall, 1983)
158. Zheltikov A M *Phys. Usp.* **47** 1205 (2004); *Usp. Fiz. Nauk* **174** 1301 (2004)
159. Zheltikov A M *Phys. Rev. A* **88** 063847 (2013)
160. Zheltikov A *Opt. Express* **28** 12302 (2020)
161. Koopman B O *Proc. Natl. Acad. Sci. USA* **17** 315 (1931)
162. Schulman L S *Techniques and Applications of Path Integration* (New York: Wiley, 1981)
163. Cohen L *Time–Frequency Analysis* (Englewood Cliffs, NJ: Prentice Hall, 1995)
164. Walmsley I A, Dorrer C *Adv. Opt. Photon.* **1** 308 (2009)
165. Voronin A A, Lanin A A, Fedotov A A, Zheltikov A M *Opt. Lett.* **43** 1327 (2018)
166. Zheltikov A M *Phys. Scr.* **90** 128003 (2015)
167. Crooks G E *Phys. Rev. Lett.* **99** 100602 (2007)
168. Gilmore R *Phys. Rev. A* **31** 3237 (1985)
169. Ruppeiner G *Phys. Rev. A* **20** 1608 (1979)
170. Weinhold F *J. Chem. Phys.* **63** 2479 (1975)
171. Schlögl F *Z. Phys. B* **59** 449 (1985)
172. Jarzynski C *Annu. Rev. Condens. Matter Phys.* **2** 329 (2011)
173. Seifert U *Annu. Rev. Condens. Matter Phys.* **10** 171 (2019)
174. Horowitz J M, Gingrich T R *Nat. Phys.* **16** 15 (2020)
175. Hasegawa Y, Van Vu T *Phys. Rev. Lett.* **123** 110602 (2019)
176. Timpanaro A M et al. *Phys. Rev. Lett.* **123** 090604 (2019)
177. Gingrich T R et al. *Phys. Rev. Lett.* **116** 120601 (2016)
178. Li J et al. *Nat. Commun.* **10** 1666 (2019)
179. Seifert U *Rep. Prog. Phys.* **75** 126001 (2012)
180. Barato A C, Seifert U *Phys. Rev. Lett.* **114** 158101 (2015)
181. Barato A C, Seifert U *Phys. Rev. X* **6** 041053 (2016)
182. Cao Y et al. *Nat. Phys.* **11** 772 (2015)
183. Mehta P, Schwab D J *Proc. Natl. Acad. Sci. USA* **109** 17978 (2012)
184. Voets T et al. *Nature* **430** 748 (2004)
185. Patapoutian A et al. *Nat. Rev. Neurosci.* **4** 529 (2003)
186. Brauchi S, Orio P, Latorre R *Proc. Natl. Acad. Sci. USA* **101** 15494 (2004)
187. Clapham D E, Miller C *Proc. Natl. Acad. Sci. USA* **108** 19492 (2011)
188. Zheltikov A M *J. Appl. Phys.* **123** 224701 (2018)
189. Zheltikov A M *J. Appl. Phys.* **123** 224701 (2018)
190. Young N P, Deisseroth K *Nature* **542** 173 (2017)
191. Lee J H et al. *Nature* **465** 788 (2010)
192. Shneider M N, Voronin A A, Zheltikov A M *J. Appl. Phys.* **110** 094702 (2011)
193. Zheltikov A M, Anokhin K *Phys. Rev. E* **84** 061902 (2011)
194. Zheltikov A M *Phys. Usp.* **61** 1016 (2018); *Usp. Fiz. Nauk* **188** 1119 (2018); *Spectrochim. Acta A* **251** 119351 (2021)
195. Walls A C et al. *Cell* **181** 281 (2020)
196. Lan J et al. *Nature* **581** 215 (2020)
197. Shang J et al. *Nature* **581** 221 (2020)
198. Yuan M et al. *Science* **368** 630 (2020)
199. Wrapp D et al. *Science* **367** 1260 (2020)
200. Vincent C et al. *Laser Phys. Lett.* **17** 076202 (2020)
201. Peng T et al., submitted
202. Rao C R *Bull. Calcutta Math. Soc.* **37** 81 (1945)
203. Cramér H *Mathematical Methods of Statistics* (Princeton, NJ: Princeton Univ. Press, 1946)
204. Ermakova Yu G et al. *Nat. Commun.* **8** 15362 (2017)
205. Clapham D E *Nature* **426** 517 (2003)
206. McKemy D D, Neuhausser W M, Julius D *Nature* **416** 52 (2002)
207. Xu H et al. *Nature* **418** 181 (2002)
208. Ramsey I S, Delling M, Clapham D E *Annu. Rev. Physiol.* **68** 619 (2006)
209. Gracheva E O et al. *Nature* **464** 1006 (2010)
210. Fedotov I V et al. *Sci. Rep.* **5** 15737 (2015)
211. Safronov N A et al. *Appl. Phys. Lett.* **106** 163702 (2015)
212. Lanin A A et al. *Opt. Lett.* **41** 5563 (2016)
213. Hille B *Ion Channels of Excitable Membranes* (Sunderland, MA: Sinauer, 2001)
214. Roshchin M et al. *Neurosci. Lett.* **687** 153 (2018)
215. Boyden E S et al. *Nat. Neurosci.* **8** 1263 (2005)
216. Deisseroth K *Nat. Meth.* **8** 26 (2011)
217. Deisseroth K *Nat. Neurosci.* **18** 1213 (2015)
218. Boyden E S *Nat. Neurosci.* **18** 1200 (2015)
219. Chung K et al. *Nature* **497** 332 (2013)
220. Kim C, Adhikari A, Deisseroth K *Nat. Rev. Neurosci.* **18** 222 (2017)
221. Lentz T B, Gray S J, Samulski R J *Neurobiol. Dis.* **48** 179 (2012)
222. Lanin A A et al. *J. Biophoton.* **13** e201900243 (2020)
223. Lanin A A et al. *J. Biophoton.* **12** e201800432 (2019)
224. Pochechuev M S et al. *J. Biophoton.* **11** e201600203 (2018)
225. Pochechuev M S et al. *J. Biophoton.* **11** e201700106 (2018)
226. Fedotov I V et al. *J. Biophoton.* **10** 775 (2017)
227. Doronina-Amitonova L V et al. *Phys. Usp.* **58** 345 (2015); *Usp. Fiz. Nauk* **185** 371 (2015)